

University of Alberta

**Study of Effects of Polymer Elasticity on Enhanced Oil Recovery by Core
Flooding and Visualization Experiments**

by

Santhosh Kumar Veerabhadrapa

A thesis submitted to the Faculty of Graduate Studies and Research
in partial fulfillment of the requirements for the degree of

Master of Science

in

Petroleum Engineering

Department of Civil and Environmental Engineering

©Santhosh Kumar Veerabhadrapa

Fall 2012

Edmonton, Alberta

Permission is hereby granted to the University of Alberta Libraries to reproduce single copies of this thesis and to lend or sell such copies for private, scholarly or scientific research purposes only. Where the thesis is converted to, or otherwise made available in digital form, the University of Alberta will advise potential users of the thesis of these terms.

The author reserves all other publication and other rights in association with the copyright in the thesis and, except as herein before provided, neither the thesis nor any substantial portion thereof may be printed or otherwise reproduced in any material form whatsoever without the author's prior written permission.

ABSTRACT

Polymer flooding is the simplest and one of the most widely used chemical Enhanced Oil Recovery (EOR) techniques. Viscoelasticity of polymers is known to contribute significantly towards improved displacement efficiency in polymer flood operations. But the contribution of elasticity of viscoelastic polymers in EOR still remains largely unexplored.

This study aims to delineate and investigate the individual effects of elasticity of partially hydrolyzed polyacrylamide (HPAM) polymer towards improved oil recovery. This was achieved by formulating polymers such that they have same average molecular weight (shear viscosity) but different molecular weight distribution (elasticity). Series of linear and radial core flooding experiments were conducted along with visual analysis.

Results from the experiments indicate that, polymer with higher elasticity gives higher recovery. Considering the molecular weight distribution together with average molecular weight seems to be a better approach for screening polymer for EOR. Elasticity of polymer solutions could well be used as a screening criterion for EOR applications.

ACKNOWLEDGEMENTS

With great pleasure and pride I express my deepest gratitude and appreciation to my supervisors Dr. Japan J. Trivedi and Dr. Ergun Kuru, whose valuable mentorship, guidance, and constant support throughout my research study has made this thesis possible.

I'm also thankful to our lab technician, Mr. Stephen Gamble for his technical support and patience. Special thanks to my dear friends Shishir Shivhare, Tolkynay Urbissinova, Shivana Samuels and Ankit Doda for helping me conduct experiments in the lab.

I'm heartily thankful to my family in India, Appaji, Amma, brother Chandan and sisters Pavithra and Chaithra for their constant love and encouragement. Thanks to my dearest friends Mudit, Rajpreet, Amit, Prarthna, Prajakta, Shree, Nikhil, Dipen and Vishnu who made my stay in Edmonton an enjoyable experience.

Financial support from Natural Sciences and Engineering Research Council of Canada (NSERC) is greatly acknowledged. Also, I'd like to thank SNF Canada for providing polymer samples at no cost.

TABLE OF CONTENTS

1. INTRODUCTION	1
1.1 Overview and Background	1
1.2 Problem Statement	5
1.3 Objectives and Methodology of the Study.....	7
1.4 Structure of the Thesis	8
2. LITERATURE REVIEW	10
2.1 Mechanism of Polymer Flooding.....	10
2.1.1 Mobility Ratio	12
2.1.2 Fractional Flow	14
2.1.3 Resistance Factor.....	15
2.1.4 Sweep Efficiency.....	16
2.2 Selection of an EOR Process and Polymer Screening Criteria.....	19
2.3 EOR Polymers	25
2.3.1 Partially Hydrolyzed Polyacrylamide (HPAM)	25
2.3.2 Advantages and Disadvantages of HPAM Polymers.....	26
2.4 Rheological Properties of Polymer Solutions	27
2.4.1 Power-Law Model.....	28

2.4.2 Carreau Model.....	30
2.4.3 Viscoelastic Models	31
2.5 Viscoelastic Polymer Flow in Porous Media.....	33
2.6 Polymer Flooding Field Projects	35
2.6.1 Daqing Oil Field.....	36
2.6.2 Polymer Flooding Projects in Canada.....	39
2.6.3 Polymer Flooding Projects Elsewhere	40
3. POLYMER SOLUTION PREPARATION AND RHEOLOGICAL CHARACTERIZATION	43
3.1 Polymer Molecular Weight and Solution Concentration.....	43
3.2 Polymer Solution Preparation	44
3.2.1 Polymers Used.....	44
3.2.2 Polymer Solution Composition	45
3.2.3 Procedure for the Preparation of HPAM Solutions.....	47
3.3 Rheological Characterization.....	49
3.3.1 Viscometry Test	50
3.3.2 Oscillation Test	51
4. CORE FLOODING EXPERIMENTS	55
4.1 Materials Used	55
4.1.1 Polymers.....	55

4.1.2 Mineral Oil	55
4.1.3 Porous Media.....	56
4.2 Experimental Setup.....	56
4.2.1 Radial Core Holder.....	57
4.2.2 Syringe Pump	58
4.2.3 Data Acquisition System.....	59
4.3 Experimental Procedure.....	60
4.3.1 Procedure for Packing the Core Holder	60
4.3.2 Porosity Measurement.....	60
4.3.3 Permeability Measurements	60
4.3.4 Flow Rate Determination	62
4.3.5 Flooding Procedure	63
5. CORE FLOODING EXPERIMENTS: RESULTS AND DISCUSSION ...	65
5.1 Rheological Characterization of HPAM Solutions.....	65
5.1.1 Viscometry Tests.....	65
5.1.2 Oscillation Tests.....	68
5.2 Core Flooding Experimental Results.....	70
5.2.1 Pressure Drop during Flooding Experiments	71
5.2.2 Oil Recovery Performance and Polymer Elasticity.....	72
5.2.3 Amount of Polymer Required	76

5.3 Changes in Rheological Characteristics of Polymer Solutions before and After Flooding.....	77
6. VISUALIZATION EXPERIMENTS	80
6.1 Overview	80
6.2 Materials Used	83
6.2.1 Polymers.....	83
6.2.2 Mineral Oil.....	83
6.2.3 Porous Media.....	84
6.3 Experimental Setup.....	84
6.3.1 Visual Cell.....	85
6.3.2 Syringe Pump	85
6.4 Experimental Procedure.....	86
6.5 Rheological Characterization of HPAM Solutions.....	87
6.6 Results and Discussion of Visualization Experiments.....	87
6.6.1 Oil Recovery Performance	87
6.6.2 Visual Analysis	90
7. CONCLUSIONS AND RECOMMENDATIONS	97
7.1 Conclusions.....	97
7.2 Recommendations.....	101
8. REFERENCES	103

LIST OF FIGURES

Fig. 1.1 – Summary of EOR mechanisms.....	3
Fig. 2.1 – Polymer flooding process	10
Fig. 2.2 – Favorable and unfavorable mobility ratio effects on displacement efficiency.....	13
Fig. 2.3 – Sweep efficiencies	17
Fig. 2.4 – Aerial sweep efficiency for a five-spot pattern waterflood process ...	18
Fig. 2.5 – Summary of EOR projects.....	21
Fig. 2.6 - Staged process for EOR project evaluation and development	22
Fig. 2.7 – Technical Screening Criteria for Polymer Flooding.....	23
Fig. 2.8 – Polymer project evaluation and development stages.....	24
Fig. 2.9 – Chemical structure of polyacrylamide (not hydrolyzed)	25
Fig. 2.10 - Molecular structure of partially hydrolyzed polyacrylamide	26
Fig. 2.11 – Flow behavior of polymer solutions	29
Fig. 2.12 – Comparison of Carreau model and Power-law model.....	31
Fig. 2.13 – Viscoelastic Polymer Flow through Porous Media	34
Fig. 2.14 – Effect of HPAM on residual oil held by capillary forces	35
Fig. 2.15 – Summary of polymer field projects	38
Fig. 2.16 – Polymer flood case histories	38
Fig. 2.17 – Polymer / ASP projects active or planned in Alberta during 2011...	40
Fig. 2.18 – Polymer flooding field case studies outside of Canada	41
Fig. 3.1 – Elga Purelab Ultra.....	47
Fig. 3.2 - Hamilton Beach overhead mixer	48

Fig. 3.3 – Bohlin Rheometer	50
Fig. 3.4 – G' and G'' vs Angular Frequency for HPAM-4.....	53
Fig. 4.1 – Schematic of the radial core flooding setup	57
Fig. 4.2 – Radial Core Holder	58
Fig. 4.3 – Constant Rate Syringe Pump	59
Fig. 4.4 – Pressure drop – Flow rate profile for water injection	61
Fig. 5.1 – Shear Stress vs. Shear Rate profiles for HPAM-1 to HPAM-7	66
Fig. 5.2 – Shear Viscosity vs. Shear Rate profiles for HPAM-1 to HPAM-7	68
Fig. 5.3 – Viscous Modulus vs. Angular Frequency for HPAM-1 to HPAM-7 .	69
Fig. 5.4 – Elastic Modulus vs. Angular Frequency for HPAM-1 to HPAM-7 ...	70
Fig. 5.5 – Pressure Drop during Polymer Flooding Experiments	71
Fig. 5.6 – Cumulative Oil Produced vs. Pore Volume of Polymer Injected	72
Fig. 5.7 – Breakthrough and Overall Oil Recovery	73
Fig 5.8 – Shear Viscosity Reduction Plots.....	78
Fig 5.9 – Viscous Modulus Reduction Plots.....	79
Fig 5.10 – Elastic Modulus Reduction Plots.....	79
Fig. 6.1 - Schematic representation of the experimental setup	84
Fig. 6.2 – Visual Cell	85
Fig. 6.3 – Chemyx Nexus Syringe Pump.....	86
Fig. 6.4 - Cumulative oil produced vs. pore volume of polymer injected	89
Fig. 6.5 - Breakthrough recovery and overall oil recovery after polymer flooding	89

Fig. 6.6 - Displacement fronts for polymer flooding at different pore volumes of polymer injected.....	91
Fig. 6.7(a) - Magnified portion of displacement fronts after injecting 0.19 PV (Left) and 0.35 PV (Right) of polymer solution	92
Fig. 6.7(b) - Magnified portion of displacement fronts after injecting 0.71 PV of polymer solution	93

LIST OF TABLES

Table 3.1 – HPAM grades and their average molecular weights.....	44
Table 3.2 – Composition and weight average molecular weights of HPAM samples.....	46
Table 4.1 – Physical properties of mineral oil (Fisher Scientific® Product Data Sheet)	56
Table 5.1 - Power law parameters of HPAM samples	66
Table 5.2 – Breakthrough and Overall Oil Recovery	74
Table 6.1 - Overall and Breakthrough recoveries after HPAM flooding.....	88

CHAPTER 1

INTRODUCTION

1.1 Overview and Background

Fast depleting oil reserves coupled with ever increasing demand for energy is pushing the modern technology, as we know today, to its brink. More than two decades ago, in an article, Menard (1981) predicted that the probability of discovering new oil fields with an oil content of more than 100 billion barrels is very low. As we are witnessing today, the rate of replacement of the produced reserves by new discoveries has been declining steadily. This scenario leads to the conclusion that the demand for oil may not only be met by putting more efforts in exploration alone but also by improving the production techniques from known and existing reservoirs.

Enhanced Oil Recovery (EOR) in recent years has gained tremendous importance due to fast depleting oil reserves worldwide. Major advances in technology and high oil prices have made more and more oil reservoirs as potential candidates for EOR applications. Improved/enhanced oil recovery comes into picture when primary and secondary recovery techniques have been applied and a considerable portion of original oil in place (OOIP) still resides in the reservoir.

Every reservoir, whether mature, recently discovered or even yet to be discovered, are all potential candidates for EOR. During the past five decades or

so, an array of improved/enhanced oil recovery methods have been developed and applied to mature and mostly depleted oil reservoirs. These methods help improve the efficiency of oil recovery by extracting a good portion of oil left behind in the reservoir after primary and secondary recovery processes. Primary recovery process involves displacing oil from porous rocks in the reservoir towards the production well using its own reservoir energy such as natural water drive, gas-cap drive or gravity drainage. Primary methods extract only about 30% to 40% of the original oil in place. In secondary recovery, a fluid (most commonly water) is injected into the reservoir in order to maintain reservoir pressure and continue oil displacement into the wellbore.

During 1950s, waterflooding became a standard practice in order to maintain reservoir pressure and also to sweep out oil in more and more reservoirs. Since then waterflooding has been studied and applied to numerous fields worldwide with variable degree of success. A significant portion of oil would still be left in the reservoir upon completion of secondary recovery. EOR methods are then aimed at recovering this residual oil. Conventional oil production strategies have followed the order of primary depletion, secondary recovery and tertiary recovery processes. Transition from one recovery method to another occurs when the current method becomes uneconomical or the oil production rate drops to very low values. However, in many cases, applying tertiary recovery methods directly after the primary depletion have proved to be more efficient. EOR aims at extracting as much recoverable oil from the reservoir as possible.

Main categories of EOR methods include gas injection, chemical flooding and thermal processes. A summary of different stages involved in EOR methods is given in **Fig. 1.1**.

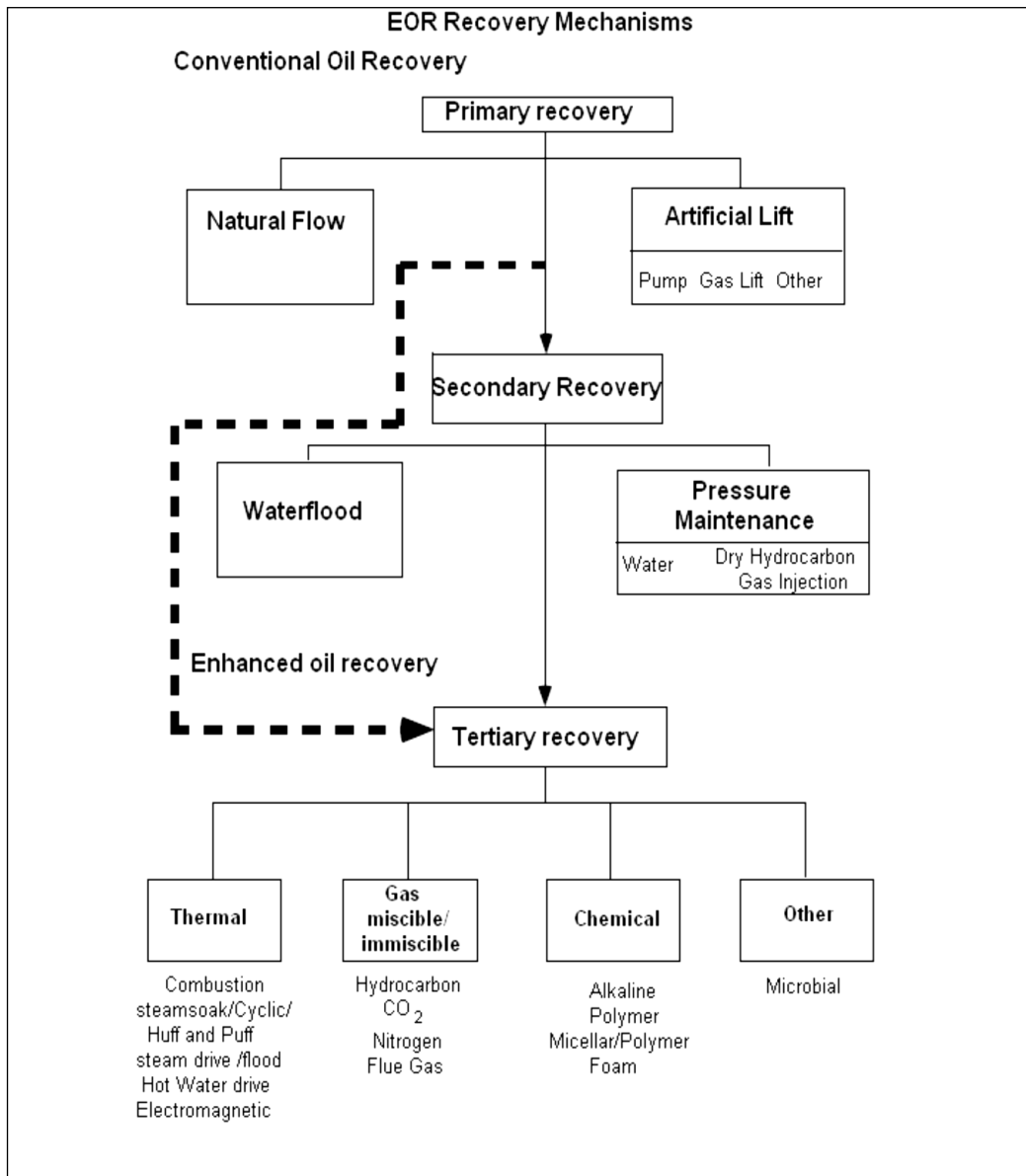


Fig. 1.1 – Summary of EOR mechanisms (Kalifa and Aluhwal, 2008)

A large percentage of oil produced nowadays worldwide is through water flooding and one of the major concerns associated with water flooding is its poor sweep efficiency. Unfavorable mobility ratio causes water to channel through oil regions leaving a considerable portion of recoverable oil in the reservoir resulting in lower oil recoveries. Efficiency of a waterflood operation can be greatly improved by lowering the water-oil mobility ratio in the system. This is achieved by adding a suitable water-soluble polymer to injected water, which increases the viscosity of the injecting fluid.

Polymer flooding is the simplest and most widely used chemical EOR technique. Ample polymer flooding projects have been conducted with different level of success ever since the technique was introduced 50 years ago. Some of the early pioneering work on polymer flood technology was done by authors such as, Pye (1964), Clay and Menzie (1966), Gogarty (1967), Armstrong (1967), Burick (1968), and Sandiford (1969). Importance of polymer flooding is evident from the fact that, currently, more oil is produced by polymer flooding than all of the other chemical EOR processes combined (Pope, 2011).

Viscoelasticity is an intrinsic property of polymer solutions exhibiting both viscous and elastic characteristics when undergoing deformation. When such viscoelastic materials are subjected to sinusoidally oscillating stress, they behave in such a way that, they fall in between the categories of a perfectly elastic solid and a perfectly viscous liquid (Ferry, 1980). A good example is the flow of

fluids in a natural reservoir where the pore channels are usually tortuous and converging/diverging. Polymer solutions flowing through such sections are subjected not only to shear but also elongation in the direction of flow. Increase in viscosity caused by the elastic response of polymer molecules is termed as elastic viscosity or simply “viscoelasticity” (Chauveteau, 1981).

Many authors in the past have reported that viscoelasticity of polymers helps to improve oil recovery in polymer flooding operations. Understanding the rheological properties and behavior of viscoelastic polymers under different reservoir conditions is very important in order to get the best out of viscoelastic polymers, which would result in better recovery performance.

1.2 Problem Statement

It is a common practice to select a polymer based on the viscosity range, concentration and average molecular weight without giving much emphasis on how the rheological characteristics of polymers actually affect the oil recovery. Recent studies, however, providing more information regarding the role of polymer solution rheology on sweep efficiency, suggested that selecting the type of polymer and understanding how its fluid rheology affects oil recovery are probably among the most critical factors that needs to be considered in designing a successful polymer flood operation. It is very important to device a general screening criterion for selecting polymers for EOR based on their rheological properties.

One key property of EOR polymers that makes polymer flooding one of the most widely used chemical EOR techniques is its viscoelasticity. Laboratory and field experiments along with numerical simulations have shown that the viscoelastic characteristics of polymer solutions help improve polymer flood efficiency (Masuda *et al.* 1992, Han *et al.* 1995, Wang *et al.* 2000, Zhang, 2007, Delshad *et al.* 2008, Dehghanpour and Kuru, 2009, Zhang *et al.* 2010). Through core flooding experiments and numerical simulation, Han *et al.* (1995) concluded that displacement efficiency of a polymer flood operation would reach its maximum when the viscoelastic property of polymer solution is brought into full play. As shown previously, extensive literature is available aimed towards understanding the role played by viscoelasticity of polymers in improving polymer flood efficiency. But the individual effect of elasticity of viscoelastic polymers on improved oil recovery remains vaguely understood. In this work, the individual effect of elasticity of partially hydrolyzed polyacrylamide (HPAM) solutions on sweep efficiency is studied by comparing the results of oil displacement by polymer solutions having similar shear viscosity but different elastic properties.

Most chemical EOR processes involve one fluid displacing another with, more-often-than-not, less viscous fluid displacing the more viscous one. Since less viscous fluid has the greater mobility, instabilities always exist. This inevitably causes viscous fingering to appear along the direction of flow. Majority of horizontal immiscible flooding experiments performed to date have described the mechanism of viscous fingering through more common governing factors

such as, viscosity ratio, capillary number difference, relative permeability, flow rate, interfacial tension etc. But what role does elasticity of polymers play, if any, in viscous fingering is a question that still needed to be answered. The role of elasticity on stability and polymer fingering has never studied before. Question such as, is there a fingering phenomenon due to difference in polymer elasticity and if so, what kind?, has not been addressed before. The effect of these probable fingers on recovery performance quantification also needs the understanding of mechanistic interpretation via visual inspection. An attempt has been made to answer these questions through core flooding experiments with visual analysis.

1.3 Objectives and Methodology of the Study

Objectives involved with this study were;

- To device a polymer screening criteria for selecting polymers, that have same average molecular weight, based on their elasticity values.
- To study the individual effect of elasticity of viscoelastic polymers on EOR
- To conduct a detailed visual analysis on frontal displacement of oil by viscoelastic polymers during polymer flooding.

The objectives were accomplished by adopting following methodology:

1. Formulating HPAM solutions such that they have same average molecular weight (i.e., same viscosity) but different molecular weight distribution (i.e., different elasticity).

2. Studying the rheological characteristics of polymer solutions such as shear viscosity, elastic modulus and viscous modulus.
3. Polymer flooding experiments using core holders specifically designed to simulate radial and linear flows.
4. Analysis of experimental results, studying the performance of each type of polymer in terms of breakthrough and overall recoveries.
5. Visual analysis of frontal displacement patterns after linear core flooding experiments.
6. Drawing conclusions based on the findings from the flooding experiments and corresponding visual analysis.

1.4 Structure of the Thesis

Chapter 1 gives a brief overview and background of enhanced oil recovery, explains the aim of the research and methodology adopted to address the problem statement.

Chapter 2 outlines a detailed literature review of main areas related to the theme of the research. It explains the concept of EOR, polymer flooding mechanism and terminologies, polymer screening criteria with several case studies and examples, structure and rheological properties of HPAM polymer, and finally a brief review of past polymer flooding field projects.

Chapter 3 provides the procedure for polymer solution preparation. Formulae involved and instruments used are explained. Methodology of polymer solution characterization is also provided.

Chapter 4 is about the radial core flooding experiments. It describes the materials, equipment and procedures for conducting radial core flooding experiments.

Chapter 5 discusses the results drawn from radial core flooding experiments. The results from rheological tests on HPAM solutions are explained. Detailed discussions on all the outcomes of radial core flooding experiments are presented.

Chapter 6 describes another set of experiments involving visual study. Concept of visualization of displacement fronts involving two immiscible fluids is explained. It describes the materials, equipment and procedure for conducting linear core flooding visualization experiments. With the help of photographs, the mechanism of viscous fingering is explained. Detailed discussion of results from rheological characterization of HPAM polymers is given.

Chapter 7 concludes the thesis with a summary of the experimental results and recommendations for further research.

CHAPTER 2

LITERATURE REVIEW

2.1 Mechanism of Polymer Flooding

Polymer flooding, also known as polymer-augmented water flooding is a chemical EOR method designed to alleviate the problems associated with conventional waterflood processes as a result of either unfavorable mobility ratio or reservoir heterogeneity.

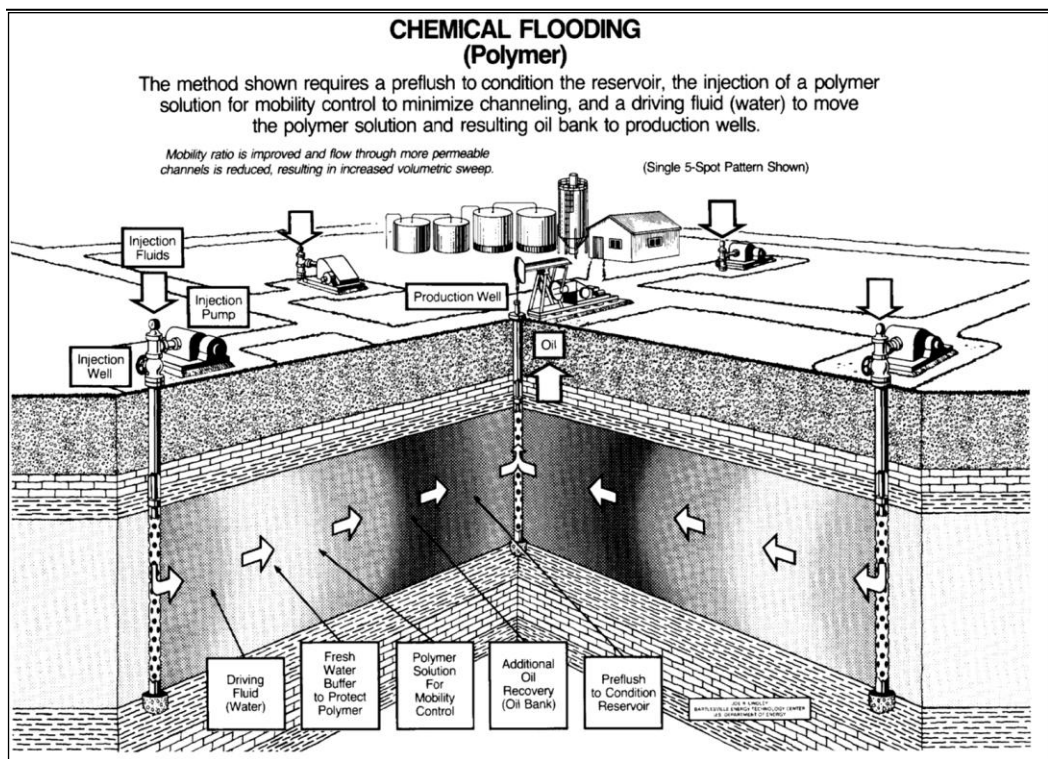


Fig. 2.1 – Polymer flooding process (Lindley, 2001)

Water soluble polymers are added to injected water to decrease water-oil mobility ratio which would lead to better sweep efficiency and also more efficient oil displacement in the swept zone (Lake, 1989). Schematic of a typical field scale polymer flood process is shown in **Fig. 2.1**.

Since oil and water are immiscible fluids, neither one can completely displace the other under reservoir conditions. Oil is left behind in the reservoir after waterflood either because it is trapped by the capillary forces (residual oil) or because it somehow gets bypassed. Residual oil trapped in the pores is immobilized due to strong capillary forces (Dullien, 1979). In order to remobilize the trapped residual oil, the interfacial tension between oil and water phases must be lowered to a sufficiently low value. This can be achieved by adding a surfactant to the injecting fluid; but recovering residual oil by this method is the aim of low-tension surfactant flooding (Lake, 1989). Polymer flooding can neither reduce the interfacial tension to sufficiently low value nor greatly increase the viscous-to-capillary force balance between water and oil phases in the displacement; without which the residual oil cannot be mobilized. Hence, the target of polymer flooding is to recover that portion of oil that is bypassed by waterflood but does not include residual oil (Sorbie, 1991). Even though polymer flooding cannot reduce the residual oil saturation (S_{or}), it still is an effective way to reach the S_{or} more quickly or more economically (Du and Guan, 2004).

Needham and Doe (1987) in their review concluded that, higher oil recovery resulting from polymer flooding over that of a conventional waterflooding could be through following three ways:

- (1) through the effects of polymer on fractional flow
- (2) by lowering water-oil mobility ratio

(3) through more efficient oil displacement in the swept zone.

In order to fully understand and appreciate the mechanism of polymer flooding, it is very essential to first gain knowledge about some of the key concepts associated with polymer flooding, such as, mobility ratio, fractional flow, types of sweep efficiency (displacement efficiency and volumetric sweep efficiency) and resistance factor.

2.1.1 Mobility Ratio

Mobility ratio, M , is the ratio of mobility of displacing fluid to the mobility of displaced fluid. It is defined for waterfloods as follows:

$$M = \frac{\lambda_w}{\lambda_o} = \frac{\left(\frac{k_w}{\mu_w} \right)}{\left(\frac{k_o}{\mu_o} \right)} \quad (2.1)$$

where,

λ_o and λ_w are the mobility of displaced fluid (oil) and the mobility of displacing fluid (water) respectively

μ_o and μ_w are the viscosities of oil and water respectively

k_o and k_w are the effective permeabilities of oil and water phases respectively.

A mobility ratio of greater than one indicates that water is more mobile than oil and it would finger through the oil zone leading to early breakthrough, consequently resulting in low displacement efficiency.

If the mobility ratio is equal to or less than one, it is considered to be favorable for displacing oil. This is where polymer flooding comes into picture. As explained earlier, mobility ratio reduction is one of the main reasons why polymer flooding improves sweep efficiency and oil recovery over waterflooding. Fig 2.2 illustrates how mobility ratio influences oil recovery.

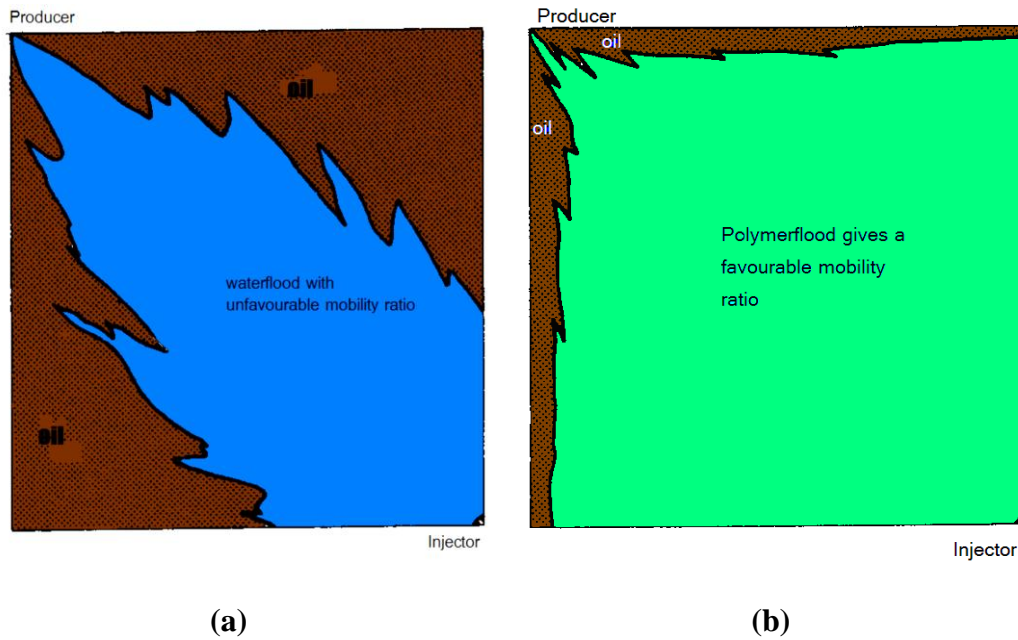


Fig. 2.2 – Favorable and unfavorable mobility ratio effects on displacement efficiency (Kalifa, O. and Aluhwal, H. 2008)

At unfavorable mobility ratios, as shown in **Fig. 2.2 (a)**, the Buckley-Leverett theory of immiscible displacement (Buckley and Leverett, 1942) predicts that the displacing fluid (water in this case), due to its higher mobility, reaches the

producer well more rapidly causing breakthrough with a considerable “tailing” period of two-phase (oil/water) production after water breakthrough. Kumar et al. (2008) performed laboratory experiments to examine the performance of waterflood with unfavorable mobility ratios. They concluded that the displacement was dominated by viscous fingering, with mobile water significantly reducing the oil recovery. They strongly recommended that, improving the mobility ratio (e.g., by adding polymer) would improve reservoir sweep and recovery efficiency considerably. When polymer is added to the injecting fluid, it effectively reduces the mobility ratio and leads to more piston-like displacement and higher recovery efficiency. This case is shown in **Fig. 2.2 (b)**.

2.1.2 Fractional Flow

Another important concept associated with two-phase immiscible flow is the fractional flow. In immiscible displacement processes, the mobility ratio does not remain constant. It varies with the saturation of the flowing phase. Assuming that water and oil are flowing simultaneously through a porous medium, the fractional flow equations for water and oil can be written as:

$$f_w = \frac{q_w}{q_w + q_o} = \frac{1}{1 + \frac{k_{ro} \mu_w}{k_{rw} \mu_o}} = \frac{1}{1 + \frac{1}{M}} \quad (2.2)$$

$$f_o = \frac{q_o}{q_w + q_o} = \frac{1}{1 + \frac{k_{rw} \mu_o}{k_{ro} \mu_w}} \quad (2.3)$$

As discussed earlier, polymer added to the injection water increases water viscosity, μ_w , and reduces the relative permeability to water (through pore blocking). As a result, the denominator in **Eq. 2.2** increases and the fractional flow of water decreases, which will improve the oil recovery performance.

2.1.3 Resistance Factor

The resistance factor is a term that is commonly used to indicate the resistance to flow encountered by a polymer solution as compared to the flow of plain water. For instance, a resistance factor of 5 means that, it is 5 times more difficult for the polymer solution to flow through the system than water. Since water has a viscosity of about 1 cp at room temperature and pressure, polymer solution, in this case, would flow through the porous medium as though it had an apparent viscosity of 5 cp even though the actual viscosity measured in a viscometer could be much lower. Resistance factor, thus, gives a good measure of the apparent viscosity of the polymer solution (Lyons, 2009).

Resistance factor, R_f , can be defined as the ratio of mobility of water to the mobility of a polymer solution (**Eq. 2.4**). The residual resistance factor, R_{rf} , is the ratio of the mobility of water before to that after the injection of a polymer solution (**Eq. 2.5**).

$$R_f = \frac{(k_w/\mu_w)}{(k_p/\mu_p)} \quad (2.4)$$

$$R_{rf} = \frac{k_w(\text{initial})}{k_w(\text{after polymer flood})} \quad (2.5)$$

The residual resistance factor is a measure of the tendency of a polymer to adsorb into the pores and thus partially block the porous medium. This indicates that resistance factor has a pronounced influence on the permeability of the porous medium. Studies done by many authors (Chauveteau 1982, Cannella *et al.* 1988, Seright 1991) have proved the permeability dependency on resistance factor through correlations. This effect, in a way, is a desired phenomenon in flooding processes as it prolongs the characteristics of the polymer flood. (Littmann, 1988).

2.1.4 Sweep Efficiency

Sweep efficiency is an important factor that, in conjunction with mobility ratio, acts as a yardstick in judging the extent of success of a flooding process. The total efficiency factor, E , represents the fraction of original oil in place at the beginning of a secondary or tertiary displacement process, that can be recovered (Craft *et al.* 1991) (Neil *et al.* 1983).

$$E = E_D \cdot E_{AS} \cdot E_{VS} \quad (2.6)$$

Where, E_D , E_{AS} and E_{VS} are displacement efficiency, aerial sweep efficiency and vertical sweep efficiency respectively. **Fig. 2.3** represents all three efficiencies in a reservoir.

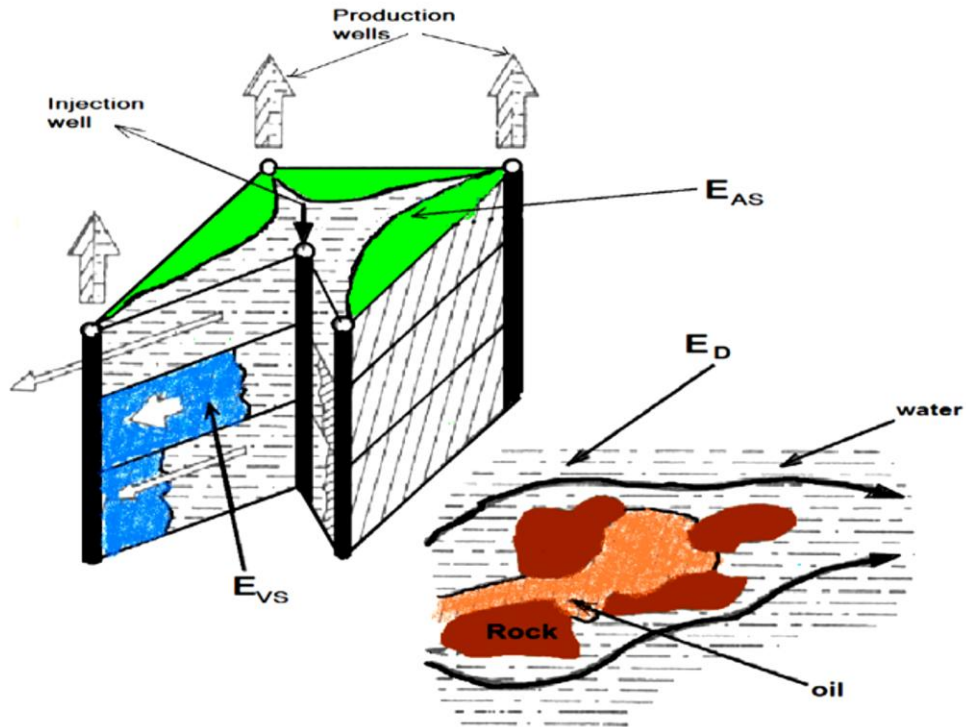


Fig. 2.3 – Sweep efficiencies (Cosse, 1993)

2.1.4.1 Displacement Efficiency (E_D)

Displacement efficiency or sometimes referred to as local or microscopic sweep efficiency is defined as the ratio of the amount of oil displaced to the amount of oil contacted by the displacing fluid (water or polymer). It is a function of the pore size distribution of the contacted volume of the reservoir and is usually estimated in waterflooding and polymer flooding operations using water saturation behind the front at the time of breakthrough (S_w) and connate water saturation (S_{wi}).

$$E_D = \frac{S_w - S_{wi}}{1 - S_{wi}} \quad (2.7)$$

2.1.4.2 Volumetric Sweep Efficiency (E_V)

Volumetric sweep efficiency is the fraction of total reservoir volume that is swept by the injected fluids. Volumetric sweep efficiency is the sum of two factors: aerial sweep efficiency and vertical sweep efficiency (**Eq. 2.8**).

$$E_V = E_{AS} + E_{VS} \quad (2.8)$$

2.1.4.3 Aerial Sweep Efficiency (E_{AS})

It is defined as the ratio of the area swept by the front to the total area. It depends on the time (volume injected), the well pattern, and also on the mobility ratio.

Fig. 2.4 represents the aerial sweep efficiencies at different stages of a waterflood operation.

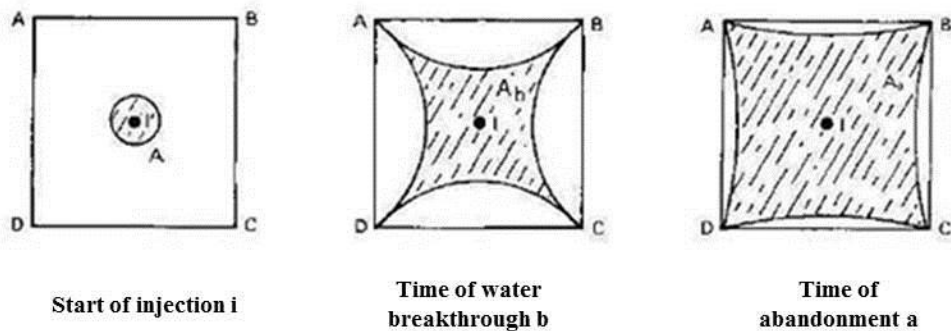


Fig. 2.4 – Aerial sweep efficiency for a five-spot pattern waterflood process

(Cosse, 1993)

For the above case, aerial sweep efficiency equations can be written as,

$$E_{ASi} = \frac{A_i}{\text{Area } ABCD} \quad E_{ASb} = \frac{A_b}{\text{Area } ABCD} \quad E_{ASa} = \frac{A_a}{\text{Area } ABCD} \quad (2.9)$$

2.1.4.4 Vertical (or invasion) Sweep Efficiency (E_{VS})

It is defined as the ratio of area swept to the total area in the vertical direction of the swept layers. It depends on the vertical heterogeneity (different permeability, strata, drains and fractures) of the reservoir and these factors hinder the regular movement of the front and are detrimental to sweep (Cosse, 1993). In many cases, vertical sweep efficiency determines the performance of a waterflood more than any other parameter.

One of the main types of heterogeneity is the large scale layering, where high-permeability strata may be laying adjacent to much lower permeability layers. This type of heterogeneity leads to early water breakthrough and hence poor vertical sweep efficiency, even if the mobility ratio is favorable (Sorbie, 1991). The role of polymer in such systems is to bring down the mobility ratio to much lower values (less than one), which improves the vertical sweep mainly as a result of viscous cross-flow effects (Clifford and Sorbie, 1985).

2.2 Selection of an EOR Process and Polymer Screening Criteria

Immediate question that arises after the primary depletion in a reservoir is; which EOR process to use and when? Providing a satisfactory answer to this question requires an integrated study of the reservoir and its characteristics. The study would typically involve answering the following basic questions:

- What is the current oil saturation?
- What is the expected residual oil saturation after waterflooding?
- What is the oil viscosity?
- What is the permeability, porosity and how heterogeneous is the reservoir?
- What type of fracturing is present in the reservoir?

After these questions are addressed, economics of the selected EOR processes must be studied in detail. Based on simplified models and detailed reservoir simulations, a decision has to be made on whether the process would be profitable or not.

Comprehensive screening guidelines for EOR techniques were provided by Aladasani and Bai (2010), and are given in **Fig. 2.5**. The table provides a range of oil and reservoir properties for various EOR methods.

Oil Properties					Reservoir Characteristics						
SN	EOR Method	# Projects	Gravity (%API)	Viscosity (cp)	Porosity (%)	Oil Saturation (% PV)	Formation Type	Permeability (md)	Net Thickness	Depth (ft)	Temperature (°F)
Miscible Gas Injection											
1	CO2	139	28[22]-45 Avg. 37	35-0 Avg. 2.1	3-37 Avg. 14.8	15-89 Avg. 46	Sandstone or Carbonate	1.5-4500 Avg. 201.1	[Wide Range]	1500 ^a -13365 Avg. 6171.2	82-250 Avg. 136.3
2	Hydrocarbon	70	23-57 Avg. 38.3	18000-0.04 Avg. 286.1	4.25-45 Avg. 14.5	30-98 Avg. 71	Sandstone or Carbonate	0.1-5000 Avg. 726.2	[Thin unless dipping]	4040[4000]-15900 Avg. 8343.6	85-329 Avg. 202.2
3	WAG	3	33-39 Avg. 35.6	0.3-0 Avg. 0.6	11-24 Avg. 18.3		Sandstone	130-1000 Avg. 1043.3	NC	7545-8887 Avg. 8216.8	194-253 Avg. 229.4
4	Nitrogen	3	38[35]-54 Avg. 47.6	0.2-0 Avg. 0.07	7.5-14 Avg. 11.2	0.76[0.4]-0.8 Avg. 0.78	Sandstone or Carbonate	0.2-35 Avg. 15.0	[Thin unless dipping]	10000[6000]-18500 Avg. 14633.3	190-325 Avg. 266.6
Immiscible Gas Injection											
5	Nitrogen	8	16-54 Avg. 34.6	18000-0 Avg. 2256.8	11-28 Avg. 19.46	47-98.5 Avg. 71	Sandstone	3-2800 Avg. 1041.7		1700-18500 Avg. 7914.2	82-325 Avg. 173.1
6	CO2	16	11-35 Avg. 22.6	592-0.6 Avg. 65.5	17-32 Avg. 26.3	42-78 Avg. 56	Sandstone or Carbonate	30-1000 Avg. 217		1150-8500 Avg. 3385	82-198 Avg. 124
7	Hydrocarbon	2	22-48 Avg. 35	4-0.25 Avg. 2.1	5-22 Avg. 13.5	75-83 Avg. 79	Sandstone	40-1000 Avg. 520		6000-7000 Avg. 6500	170-180 Avg. 175
8	Hydrocarbon + WAG	14	9.3-41 Avg. 31	16000-0.17 Avg. 3948.2	18-31.9 Avg. 25.09	Avg. 88	Sandstone or Carbonate	100-6600 Avg. 2392		2650-9199 Avg. 7218.71	131-267 Avg. 198.7
(Enhanced) Waterflooding											
9	Polymer	53	13-42.5 Avg. 26.5	4000 ^b -0.4 Avg. 123.2	10.4-33 Avg. 22.5	34-82 Avg. 64	Sandstone	1.8 ^c -5500 Avg. 834.1	[NC]	700-9460 Avg. 4221.9	74-237.2 Avg. 167
10	Alkaline Surfactant Polymer (ASP)	13	23[20]-34[35] Avg. 32.6	6500 ^c -11 Avg. 875.8	26-32 Avg. 26.6	68[35]-74.8 Avg. 73.7	Sandstone	596[10]-1520	[NC]	2723-3900[9000] Avg. 2984.5	118 [80]-158[200] Avg. 121.6
11	Surfactant + P/A	3	22-39 Avg. 31	15.6-3 Avg. 9.3	16-16.8 Avg. 16.4	43.5-53 Avg. 48	Sandstone	50-60 Avg. 55	[NC]	625-5300 Avg. 2941.6	122-155 Avg. 138.5
Thermal/Mechanical											
12	Combustion	27	10-38 Avg. 23.6	2770-1.44 Avg. 504.8	14-35 Avg. 23.3	50-94 Avg. 67	Sandstone or Carbonate [Preferably Carbonate]	10-15000 Avg. 1981.5	[>10]	400-11300 Avg. 5569.6	64.4-230 Avg. 175.5
13	Steam	271	8-30 Avg. 14.5	5E6-3 ^d Avg. 32971.3	12-65 Avg. 32.2	35-90 Avg. 66	Sandstone	1 ^e -15000 Avg. 2605.7	[>20]	200-9000 Avg. 1643.6	10-350 Avg. 105.8
14	Hot Water	10	12-25 Avg. 18.6	8000-170 Avg. 2002	25-37 Avg. 31.2	15-85 Avg. 58.5	Sandstone	900-6000 Avg. 3346	-	500-2950 Avg. 1942	75-135 Avg. 98.5
15	[Surface Mining]	-	[7] - [11]	[Zero cold flow]	[NC]	[>8 wt% Sand]	[Mineable tar sand]	[NC]	[>10]	[> 3:1 overburden to sand ratio]	[NC]
Microbial											
16	Microbial	4	12-33 Avg. 26.6	8900-1.7 Avg. 2977.5	12-26 Avg. 19	55-65 Avg. 60	Sandstone	180-200 Avg. 190	-	1572-3464 Avg. 2445.3	86-90 Avg. 88
The following reported EOR reservoir characteristics have extreme values that impact the respective average and range in Table 1.											
a – Minimum CO ₂ miscible flooding depth reported in Salt Creek Field, U.S.A. ¹⁴											
b – Maximum polymer flooding viscosity reported in Pelican Lake, Canada. ¹⁴											
c – Maximum ASP flooding viscosity reported in Lagomar, Venezuela. ¹²											
d – Maximum steam Injection viscosity reported in Athabasca Oil Sands, Canada. ¹⁴											
e – Minimum steam Injection permeability reported in North Midway-Sunset, U.S.A. ¹⁴											

Fig. 2.5 – Summary of EOR projects (Aladasani and Bai, 2010)

Kaminsky *et al.* in 2007 suggested a staged process for EOR project evaluation and development (**Fig. 2.6**).

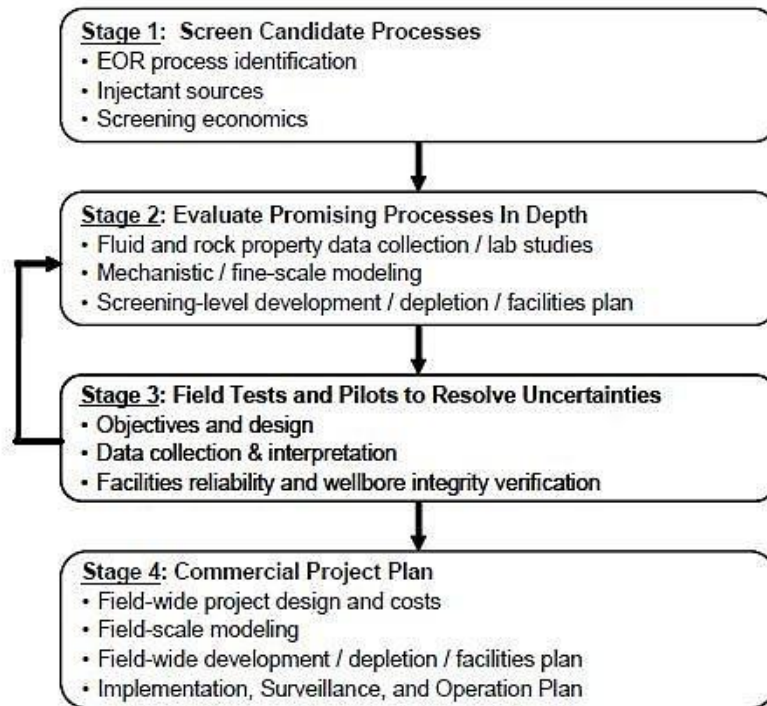


Fig. 2.6 - Staged process for EOR project evaluation and development
(Kaminsky *et al.*, 2007)

After a decision to go ahead with the polymer flooding is made, the next step would be to screen and evaluate all possible EOR polymers. Because not all polymers are suitable for every reservoir, it is very important to conduct a detailed feasibility analysis before selecting a polymer for the given reservoir conditions.

Detailed screening criteria for polymers are given in **Fig. 2.7**.

Description					
The objective of polymer flooding is to provide better displacement and volumetric sweep efficiencies during a waterflood. In polymer flooding, certain high-molecular-weight polymers (typically polyacrylamide or xanthan) are dissolved in the injection water to decrease water mobility. Polymer concentrations from 250 to 2,000 mg/L are used; properly sized treatments may require 25 to 60% reservoir PV.					
Mechanisms					
Polymers improve recovery by (1) increasing the viscosity of water; (2) decreasing the mobility of water; and (3) contacting a larger volume of the reservoir.					
Technical Screening Guides*					
	Wide-Range Recommendation			Range of Current Field Projects	
Crude Oil					
Gravity, °API	>15			14 to 43	
Viscosity, cp	<150 (preferably <100 and >10)			1 to 80	
Composition	Not critical				
Reservoir					
Oil saturation, % PV	>50			50 to 92	
Type of formation	Sandstones preferred but can be used in carbonates				
Net thickness	Not critical				
Average permeability, md	>10 md**			10 to 15,000	
Depth, ft	<9,000 (see Temperature)			1,300 to 9,600	
Temperature, °F	<200 to minimize degradation			80 to 185	
Properties of Polymer-Flood Field Projects					
Property	1980's median (171 projects)	Marmul	Oerrel	Courtenay	Daqing
Oil/water viscosity ratio at reservoir temperature	9.4	114	39	50	15
Reservoir temperature, °F	120	115	136	86	113
Permeability, md	75	15,000	2,000	2,000	870
% OOIP present at startup	76	≈92	81.5	78	71
WOR at startup	3	1	4	8	10
HPAM concentration, ppm	460	1,000	1,500	900	1,000
lbm polymer/acre-ft	25	373	162	520	271
Projected IOR, % OOIP	4.9	25***	≈13	30	11
Projected bbl oil/lbm polymer	1.1	1.2	≈1.4	0.96	0.57
Projected bbl oil/acre-ft	27	461	≈230	499	155
Limitations/Problems					
See text for limitations and recommendations for overcoming problems.					
*These screening guides are very broad. When identifying polymer-flood candidates, we recommend the reservoir characteristics and polymer-flood features be close to those of the four successful projects at the bottom of table.					
**In reservoirs where the rock permeability is less than 50 md, the polymer may sweep only fractures effectively unless the polymer molecular weight is sufficiently low.					
***IOR over primary production for this case only. For the others, IOR is incremental over waterflooding.					

Fig. 2.7 – Technical Screening Criteria for Polymer Flooding (Taber *et al.*, 1997)

Polymer screening is only the first step in a polymer flooding project. After the preliminary screening is done, a detailed project evaluation and development follows. Kaminsky *et al.* in 2007 has outlined a staged process for polymer flood project evaluation and development and is given in **Fig. 2.8**.

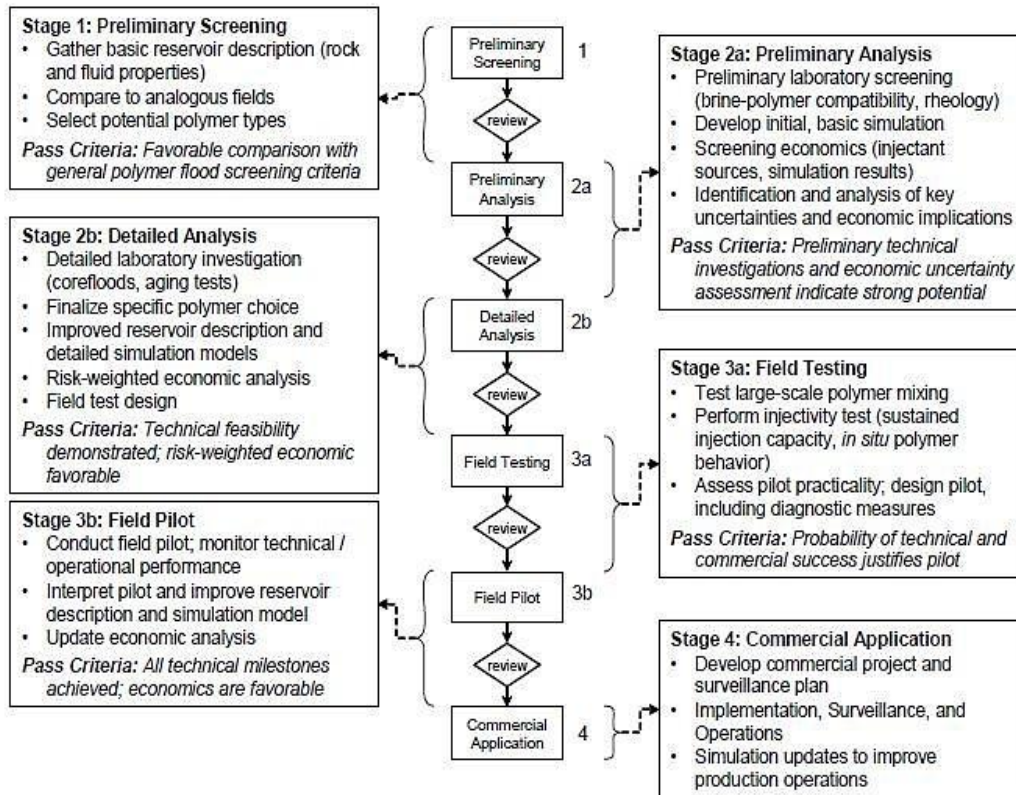


Fig. 2.8 – Polymer project evaluation and development stages (Kaminsky *et al.*, 2007)

The first stage of this extensive process is preliminary screening, where based on the reservoir rock and fluid properties and data from similar fields, a potential candidate polymer for the given field is selected. The first stage is followed by preliminary analysis and detailed analysis, both comprising Stage 2 of the process. Here, through laboratory screening, rheology studies, computer simulations and economic evaluations, the suitability of the polymer under study is assessed. The next stages include field testing, field pilot and, finally, commercial application.

2.3 EOR Polymers

Two of the most general types of polymers used in EOR processes are the synthetic polymers - polyacrylamides in their partially hydrolyzed form, referred to as HPAM, and the biopolymer - xanthan. Within the scope of this thesis, only HPAM has been discussed in detail.

2.3.1 Partially Hydrolyzed Polyacrylamide (HPAM)

Polyacrylamides are water soluble polymers used in polymer flood applications in its hydrolyzed form. Polyacrylamides are the co-polymers of acrylic acid and acrylamide. HPAM is a straight chain polymer that has acrylamide molecules as monomers as shown in **Fig. 2.9**.

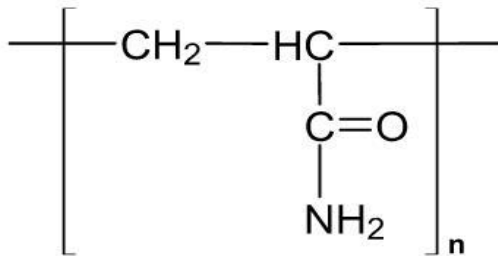
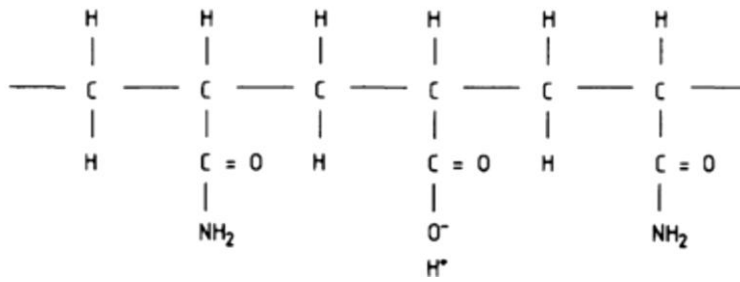


Fig. 2.9 – Chemical structure of polyacrylamide (not hydrolyzed)

Polyacrylamides used in flooding undergo partial hydrolysis, which causes the negatively charged carboxylic group (-COO-) to be scattered along the backbone of the chain. Typical degrees of hydrolysis are 25 - 35 % of the acrylamide monomers; that are chosen to optimize the specific properties of polymer solutions such as, viscosity, solubility and retention. If the degree of hydrolysis

is too small, the polymer will not be water soluble. If it is too large, its properties are very sensitive to salinity and hardness (Shupe, 1981). Molecular structure of partially hydrolyzed polyacrylamide is shown in **Fig. 2.10**.



**Fig. 2.10 - Molecular structure of partially hydrolyzed polyacrylamide
(Littmann, 1988)**

The viscosity-increasing feature of HPAM polymers is derived from the repulsive forces between polymer molecules and between the segments of the same molecule. This repulsion causes the molecules to lengthen and snag on other molecules, thus causing the viscosity to increase.

2.3.2 Advantages and Disadvantages of HPAM Polymers

HPAM polymers are inexpensive, readily available in different forms to suit the need, excellent viscosifier and more bacteria resistant than biopolymers.

But they cannot be used in waters of high salinity, especially at raised temperature; HPAM polymers are more susceptible to mechanical and shear degradation. Other disadvantages associated with HPAM are low thermal and

shear stability, injectivity problems when high molecular weight and high concentration solutions are used for flooding. Polyacrylamides degrade or precipitate in very high-temperature, high-salinity reservoirs (Akstinat, 1980; Davison and Mentzer, 1980).

New class of synthetic polymers and associative polymers with improved properties have been developed and introduced to oilfield applications to minimize problems associated with conventional polymers (polyacrylamide and xanthan). More detailed discussion and further references on new type of polymers are given elsewhere; Stahl and Schulz (1988), Caram *et al.* (2006), Lara-Ceniceros *et al.* (2007), Aktas *et al.* (2008), Buchgraber (2008), Pancharoen (2009) and so on.

2.4 Rheological Properties of Polymer Solutions

For Newtonian fluids, shear stress (τ) is directly proportional to shear rate (γ) and the proportionality constant is called the viscosity (μ) of the fluid. The simple relationship is given in **Eq. 2.10**.

$$\tau = \mu \cdot \gamma \quad (2.10)$$

There are many classes of fluids for which the viscosity does not remain constant at different rates of deformation (shear rates). This may be denoted as given in **Eq. 2.11**.

$$\tau = \eta(\gamma)\gamma \quad (2.11)$$

where, η is a viscosity function that depends on the shear rate. This is known as a material function (Bird *et al.* 1987). Fluids that show this type of behavior are known as non-Newtonian fluids.

Polymer solutions generally show non-Newtonian flow behavior at sufficiently high polymer concentrations. Several models have been proposed by different authors to explain the flow behavior of polymer solutions under different conditions (Christopher and Middleman, 1965; McKinley *et al.* 1966; Savins, 1969; van Poollen and Jargun, 1969; Hirasaki and Pope, 1974; Abou-Kassem and Ali, 1986; Pruess and Witherspoon, 1991 and so on). Most relevant ones in the context of this thesis are outlined briefly here.

2.4.1 Power-Law Model

Polymer solutions are generally pseudoplastic or shear thinning in nature, i.e. the viscosity of polymer solutions decreases with increasing shear rates. This is due to uncoiling and alignment of polymer chains when subjected to shearing. This applies to solutions of both bio and synthetic polymers – xanthan and polyacrylamide. However, the flow of biopolymers in porous media differs from that of polyacrylamides. Solutions of biopolymers show Newtonian behavior at sufficiently low flow rates, then the flow changes from Newtonian to shear thinning at increasing flow rates. The behavior of polyacrylamide is even more complex: it changes from Newtonian flow via shear thinning into shear

thickening (or dilatant, i.e. viscosity increases with increasing shear rates) beyond a certain critical flow rate.

Heemskerk *et al.* proposed a model to explain this behavior of polymer solutions and is shown in **Fig. 2.11**,

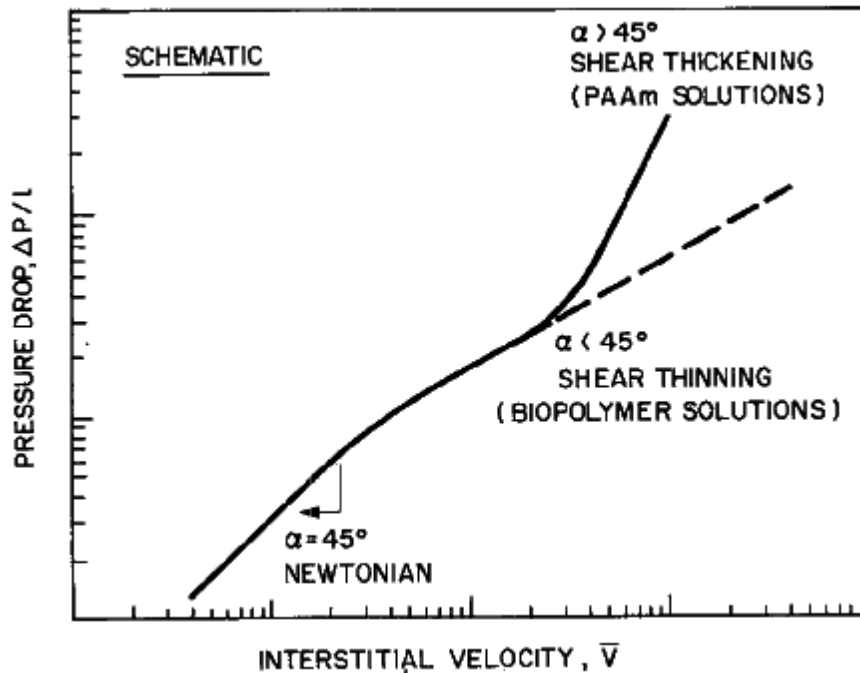


Fig. 2.11 – Flow behavior of polymer solutions (Heemskerk *et al.* 1984)

Power-law model, without doubt, is the most commonly encountered analytical form of the viscosity-shear rate relationship which describes the pseudoplastic region (Bird *et al.* 1960) and is given by the **Eq. 2.12**,

$$\tau = K \cdot \gamma^n \quad (2.12)$$

where,

τ is shear stress

γ is shear rate

K is consistency index

n is power-law index

In pseudoplastic region, n is usually less than or equal to 1 (typically $n = 0.4 - 0.7$). For a Newtonian fluid, $n = 1$ and K is simply the constant viscosity, μ .

2.4.2 Carreau Model

Drawback with power-law model is that, it can be accurately applied only within a certain range of shear rates, and not suitable at very low or high shear rates. Carreau model gives a better representation of flow behavior in these shear regimes (Carreau *et al.* 1979, Bird *et al.* 1987).

In this model, the viscosity function is given by:

$$\eta(\gamma) = \eta_{\infty} + (\eta_0 - \eta_{\infty})[1 + (\lambda\gamma)^2]^{(n-1)/2} \quad (2.13)$$

where:

η is the viscosity at the shear rate γ

η_0 is the zero shear rate Newtonian viscosity

η_{∞} is the high shear rate Newtonian viscosity

$(n-1)$ is the slope of the power-law portion of the data

λ is the time constant

Fig. 2.12 shows the improved behavior of Carreau model compared with the power-law model. Many researchers have reported that the Carreau model gives

a better fit to their viscosity/shear rate data (Abdel-Khalik *et al.* 1974; Bird *et al.* 1974; Chauveteau and Zaitoun, 1981).

Even though the Carreau model offers much better fit to the viscometry data over a wide range of shear rates, it required four parameters instead of two as in case of the power-law model. Also, the analytical calculations involving the viscosity function gets more complicated in this model.

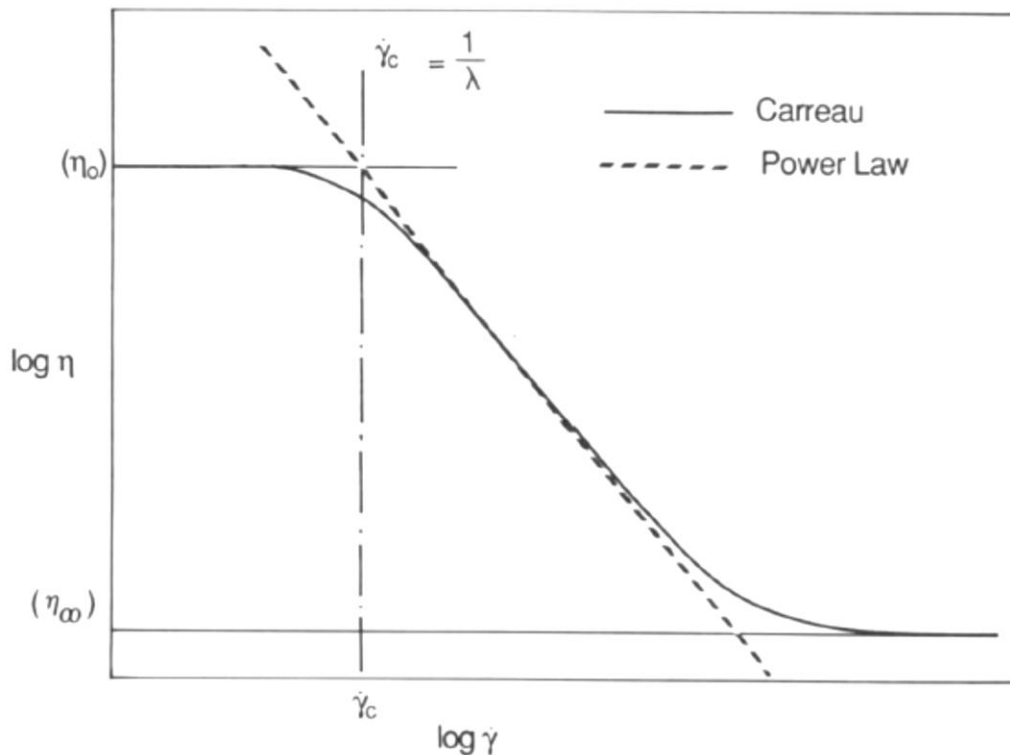


Fig. 2.12 – Comparison of Carreau model and Power-law model (Sorbie, 1991)

2.4.3 Viscoelastic Models

In the models described above, the shear-dependent fluids considered were assumed to be non-elastic. However, some polymer solutions show elasticity to

variable extents. By definition, when an elastic substance is deformed through a small displacement, it tends to return to its original configuration.

van Poollen and Jargon (1969), Willhite and Uhl (1986) and many other authors have suggested simple empirical models to account for non-linear relationship between pressure drop and the flow rate for non-Newtonian fluid flow. But these models fall short in accounting for the elastic phenomena manifested by polymer flow in porous media. Following models account for the viscous and elastic characteristics of polymer fluids.

Maxwell's Model

When a shear is applied to an ideal solid, according to Hooke's law, the displacement, which is the strain, γ , is proportional to the applied stress;

$$\tau = G'\gamma \quad (2.14)$$

where, G' is the elastic modulus of the material.

Hooke's law for ideal solids (**Eq. 2.14**) is analogous to Newton's law for the stress of a fluid.

For a fluid that has both viscous and elastic behavior (viscoelastic fluid), the equation must incorporate both these laws – Newton's and Hooke's. Maxwell came up with a model that accounted for both viscous and elastic components.

The relationship is as follows:

$$\tau_{yx} + \frac{\eta}{G'} \left(\frac{\partial \tau_{yx}}{\partial t} \right) = -\eta \gamma_{yx} \quad (2.15)$$

The above equation reduces to that for a simple Newtonian fluid under steady shear flow condition. The Maxwell model is the simplest of a very wide class of viscoelastic models. It only applies to small deformations, as it is a linear model (Sorbie, 1991).

Savins (1969), Thurston et al. (1981), Heemskerk et al. (1984), Wreath et al. (1990), Sorbie (1991), Ranjbar et al. (1992), Garrouch (1999), Garrouch and Gharbi (2006) have also proposed different viscoelastic models for polymeric solutions.

2.5 Viscoelastic Polymer Flow in Porous Media

As explained by Garrouch and Gharbi (2006), the flow of polymers in porous media deviates from Darcy's law because:

- Viscosity of polymers depends on shear rate
- Length of polymeric molecules can be comparable to the pore throat length, which imparts certain elastic properties in them
- Molecular adsorption and mechanical entrapment of polymers in porous media alter the geometry of the media, in turn altering the permeability of the media.

Viscoelastic polymer flow in porous media is different from the flow of Newtonian fluids. As shown in **Fig. 2.13**, polymers undergo a series of contractions and expansions as they flow through porous media.

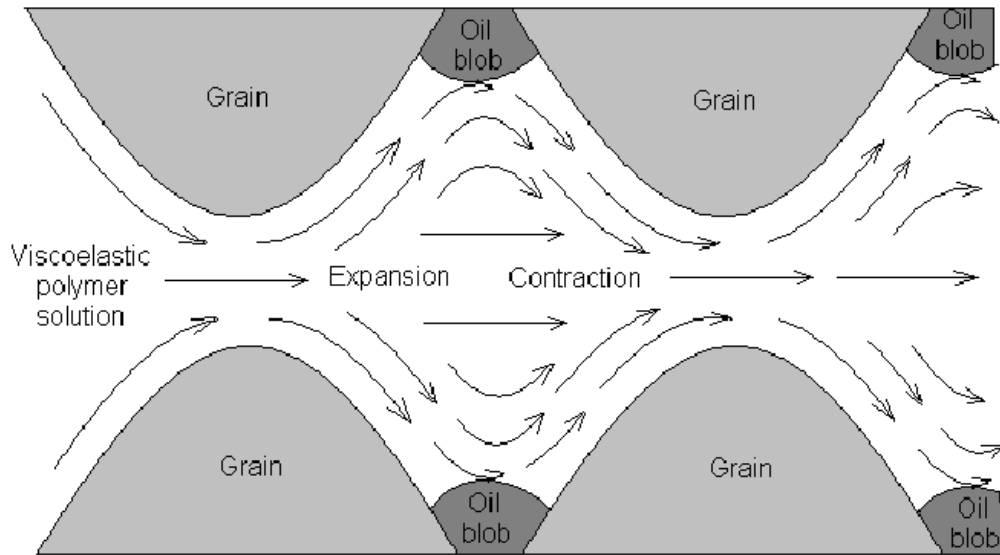


Fig. 2.13 – Viscoelastic Polymer Flow through Porous Media (Urbissinova, 2010)

Due to the continuous stretching and recoiling of polymeric molecules as they flow through porous media, they develop additional “elastic viscosity” which improves the microscopic sweep efficiency. Through micro-seepage polymer flooding experiments, Guo (1990) concluded that additional oil recovery was observed due to greater shear stress between polymer-oil than between water-oil. Zhang (2007, 2008) used constricted/expanded channels to model the pore throat in porous media and numerically studied the flow of viscoelastic polymer solution in pore throat model. It was found that smaller throat size leads to greater “elastic viscosity” and higher flow resistance. The micro-swept coefficient rises with the increase of “elastic viscosity”. Viscoelastic polymers can penetrate deep into the rock pores and efficiently displace oil; thus improving the overall oil recovery and reducing residual oil saturation.

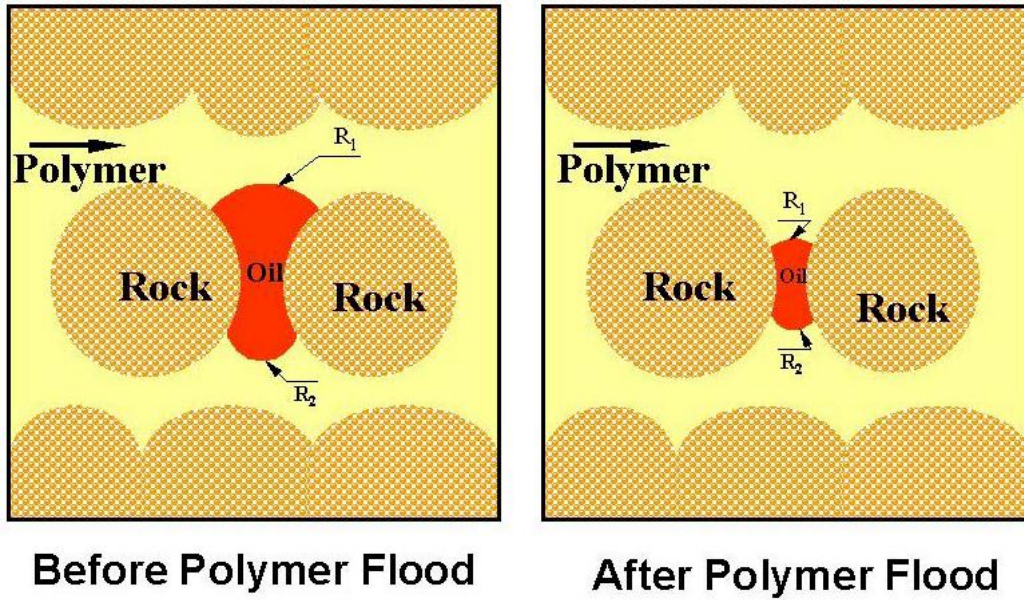


Fig. 2.14 – Effect of HPAM on residual oil held by capillary forces (Wang *et al.* 2000)

Fig. 2.14 shows how HPAM flooding reduces the residual oil trapped in pore throats held by capillary forces. The residual oil can be reduced mainly because; the oil blob is “pulled” away from both ends at the same time by the viscoelastic polymeric fluid and polymer reduces the capillary forces holding the oil droplet in the pore throat. The wettability also plays a major role in driving oil out, as driving oil from more water-wet rock surfaces is easier than driving oil from an oil-wet rock surface.

2.6 Polymer Flooding Field Projects

Numerous polymer flooding field projects have been tried with variable degree of success all around the world since the 1950s. This section contains extracts

from many review papers on some of the major polymer flood field projects that have been carried out so far.

2.6.1 Daqing Oil Field

Daqing oil field in northern China is one of the biggest oil fields in the world and produces more than 900,000 bbl/day of oil from multiple reservoirs. Commercial production from the field started in 1959 and from 1976 to 1996, the field maintained a relatively stable oil production of 1 million bbl/day. But steady decline in production has forced the field to adopt EOR techniques including polymer flooding (Yang *et al.* 2006).

Industrial scale polymer flooding was started in 1996. The lithology of the reservoir is sandstone layers with average depth 3934 feet, pay zone thickness 328 to 393 feet, permeability value varying from 50 to 5000 mD, porosity value varying from 20 to 30% and reservoir temperature is 113°F, oil viscosity is about 9-10cp, water reservoir salinity is from 5000 to 7000 ppm which considered no high salinity, injection polymer solution with concentration from 500 to 2500 ppm, finally the average incremental oil recovery is about 15% (Wang *et al.*, 2002; Lu *et al.*, 2006).

Highlights of Daqing polymer flood project:

- In the year 2004, in Daqing alone, there were 31 commercial scale projects involving 2,427 injection wells and 2,916 production wells over an area of 67,759 acres.

- An incremental oil recovery of 6 to 12% OOIP has been reported in Daqing and Shengli fields (Chang *et al.* 2006). These two fields contributed an oil production of 73.5 million barrels for the year 2004.
- Polymer flooding significantly reduced the water consumption per m³ of oil produced (by 21.8 m³).

Similar field applications were studied and summarized in **Fig. 2.15** (Kalifa and Aluhwal, 2008).

Proj No.	Field	Ref.	Lithology and area (acer)	Depth Ft	h ft	ϕ %	K mD	T F °	μ_o cp	Cp. ppm	Water salinity ppm	slug size pv	oil Rec. %
1	Daqing oil field, china	69, 43	Sandstone	3934	328 to 393	20 to 30	50 to 5000	113	9-10	500 to 2500	5000 to 7000	0.6	15
2	La-Sa-Xing Oil Field china	43	sandstone	2011 to 5614	-	17 to 27	2000	117 to 128	8 to 10	-	5000 to 7000	-	10
3	Taber Maniville south	46,45	Sandstone	3230	-	26	2107	95	58	360 to 500	-	0.20	2
4	Sleepy Hollow field in Oklahoma (Simulation)	47	Sandstone 640	-	11	24	2580	100	24	750	718	0.48	8
5	Brelum, Duval County, TX	48,45	Sandstone 265	1950	10	29.3	399	112	9.8	389	-	0.25	8.6
6	North Burbank, osage County, OK	49,45	Sandstone 160	3000	37 to 50	11 to 12	1000 to 2000	118	3	250	1200	0.18	1.6
7	Marmul oil filed, Oman	50	Sandstone	960	20	30	15000	115	80	1000	3000	0.63	25
8	Taber Mannville D Pool Field	45	Sandstone	3140	-	23	1920	92	54	250	-	0.20	-
9	West Semlek, Crook County, WY	45,51	Sandston 348	7240	27	20	647	144	12.3	200	7750	0.15	4.4
10	Angsi field core samples, Malaysia	52	Sandstone	6700	-	28	400	246	0.3	500 to 750 ASP	-	-	28

Proj No.	Field	Ref.	Lithology and area (acer)	Depth Ft	h ft	ϕ %	K mD	T F ^o	μ O cp	Cp. ppm	Water salinity ppm	slug size pv	oil Rec. %
11	North Stanley Stringer	46,45	Sandstone	2900	-	18	300	105	2.2	100 to 600	-	.024 to .07	1.1
12	East Coalinga, Fresno County, CA	45,53	Sandstone 132	1900 to 2400	125 to 350	26.5	50 to 480	100	24	500	710	-	2.8
13	Varnon, woodson County, KS	45	Sandstone 15	1000	23	20.4	23 to 29	75	75	454	-	0.33	8.6
14	Huntington Beach Orange County, CA	45	Turbidite 900	2350	53	34	2300	125	76	500	500	0.3	4.1
15	Skull Creek Western County, WY	45,70	Sandstone 555	3300	18	14.4	70	124	3.2	240 to 500	-	.034	8.2
16	Saetu field, China	71	Sandstone 773	2295 to 3934	44	25	870	113	9	570	7000	0.17	12

Fig. 2.15 – Summary of polymer field projects (Kalifa and Aluhwal, 2008)

Needham and Doe in 1987 summarized the results from early polymer flood field projects and is given in **Fig. 2.15**.

Project	Reference	Flood Type	Starting WOR	Lithology	Polymer/Water Type	Amount of Polymer Used (lbm/acre-ft)	Recovery (% OOIP)
Northeast Hallsville	2	Secondary	<1	Carbonate	Polyacrylamide/fresh	12	13
Vernon	2	Secondary	<1	Sandstone	Polyacrylamide/salt*	136	30
Huntington Beach	2	Secondary	1	Sandstone	Polyacrylamide/fresh	26	4
Brea Olinda	2	Secondary	1.2	Sandstone	Polyacrylamide/fresh	*	*
Taber Manville South	2	Secondary	1	Sandstone	Polyacrylamide/*	20	2
Skull Creek South	2	Secondary	0	Sandstone	Polyacrylamide/fresh*	32	8
Brelum	2	Secondary	<1	Sandstone	Polyacrylamide/fresh*	70	9*
Wilmington	2	Secondary	*	*	*	*	0
North Burbank	2,8	Tertiary	100	Sandstone	Polyacrylamide* */fresh	63	2.5
North Alma Penn	2	Secondary	3	Sandstone	Biopolymer/salt	18	*
Pembina	2	Secondary	9	Sandstone	Polyacrylamide/fresh	22	0
West Semlek	2,4	Secondary	0	Sandstone	Polyacrylamide/fresh	6	5
North Stanley	2,5	Tertiary	70	Sandstone	Polyacrylamide/fresh	25	1.1
West Yellow Creek	2,6	Secondary	3	Sandstone	Polyacrylamide/fresh	*	*
East Coalinga	2,7	Secondary	9	Sandstone	Biopolymer/*	2	0
Skull Creek Newcastle	9	Secondary	3	Sandstone	Polyacrylamide/fresh	28	10
Sage Spring Creek Unit A	10	Secondary	<1	Sandstone	Polyacrylamide* */fresh	5	1.2
Eliasville Caddo	11	Tertiary	32	Carbonate	Polyacrylamide/fresh	56	1.8
Chateaufrenard	12	Secondary	9	Sandstone	Polyacrylamide/fresh	188*	2.5*
Storms Pool	13	Tertiary	*	Sandstone*	Biopolymer/*	100*	0*
Oerrel	14	Secondary	4	Sandstone	Polyacrylamide/fresh	46	23
Hankensbuettel	14	Secondary	5	Sandstone	Polyacrylamide/fresh	*	13
Owasco	15	Secondary	<1	Sandstone	Polyacrylamide/fresh	21	7
Stewart Ranch	4	Secondary	1	Sandstone	Polyacrylamide/fresh	25	8
OK	4	Secondary	*	Sandstone	Polyacrylamide* */fresh*	16	3
Hamm	4	Secondary	1	Sandstone	Polyacrylamide* */fresh*	21	9
Kummerfeld	4	Secondary	*	Sandstone	Polyacrylamide* */fresh*	7	6

* Information uncertain or unavailable.
** Crosslinked flood.

Fig. 2.16 – Polymer flood case histories (Needham and Doe, 1987)

One interesting thing to note from the field cases considered in **Fig. 2.15** is that, out of 27 field cases studied, 23 were secondary operations initiated at early stages of waterflooding. From the collective summary of all the field applications, the authors concluded that polymer flooding has much greater potential as a secondary process than as a tertiary process. The recovery averages presented in the **Fig. 2.16** indicate roughly four times the potential recovery for a secondary process compared to a tertiary flood.

2.6.2 Polymer Flooding Projects in Canada

In Canada, the earliest polymer flood project was the Taber South Mannville B project in southern Alberta, beginning in 1967 (Lozanski and Martin, 1970; Shaw and Stright, 1977).

Talisman conducted a polymer flooding project at Rapdan in Southwest Saskatchewan in 1986. By 1994, the oil-cut increased by 8% and oil production rate increased from 8 to 28 m³/day (Pitts *et al.* 1995).

Many of the other projects include: Husky's ASP project in the Taber area (Anonymous, 2006; Collison, 2007), Pengrowth's polymer project in East Bodo (Wassmuth *et al.* 2009), CNRL's past and present projects (Roche, 2010), and most recently by Cenovus at Pelican Lake (Roche, 2010).

A list of all polymer or ASP projects that are active or planned during 2011 is given in **Fig. 2.17** (Singhal, 2011).

Company	Formation	Field Name	Injection Type
Blackpearl Resources Ltd.	Bluesky A	Mooney	ASP Flood
Harvest Operations Corp.	Upper Mannville U	Suffield	Polymer Flood
Cenovus Energy	Sparky JJ	Viking-Kinsella	Polymer Flood
Cenovus Energy	Upper Mannville H	Countess	Chemical Flood
Cenovus Energy	Upper Mannville UU	Suffield	ASP Flood
Harvest Operations Corp.	Wainwright B	Viking-Kinsella	Polymer Flood
Husky Oil Operations	Glauconitic K	Taber	ASP Flood
Penngrowth Energy	Lloydminster SS	Provost	Not Specified
Husky Oil Operations	Mannville B	Taber South	Polymer Flood
CNRL	Glauconitic SS	Grand Forks	Not Specified
Cenovus Energy	Upper Mannville YYY	Suffield	ASP Flood
CNRL	Athabasca Oil Sands Area	Oil Sands Area	Polymer Flood
Murphy Oil Company Ltd.	Peace River Oil Sands Area	Oil Sands Area	Polymer Flood
Enermark Inc.	Lloydminster A, Sparky E	Wildmere	Polymer Flood

Fig. 2.17 – Polymer / ASP projects active or planned in Alberta during 2011
(Singhal, 2011)

2.6.3 Polymer Flooding Projects Elsewhere

Previous experiences of polymer flooding has been reviewed and summarized by Shehata *et al.* 2012, and is given in **Fig. 2.18**.

Field	Lithology	Depth, ft	h, ft	ϕ %	K, mD	T, F°	μ_o , cp	Polymer Concentration, ppm	Water Salinity, ppm	Slug Size, pv	R.F. %
Dalia Field, Angola	Sandstone	*	328 to 393	25	100 to 6000	118	11	700	25000	*	3 to 7
Sleepy Hollow field, Oklahoma	Sandstone	*	11	24	2580	100	24	750	718	0.48	8
Niger Delta Field, Nigeria	Sandstone	*	*	39	100 to 6000	130	16	500 to 1500	20000	*	7
Marmul Field, Oman	Sandstone	960	20	30	15000	115	80	1000	3000	0.63	15
Bohai Bay - China	Sandstone	1900 to 2400	125	26.5	50 to 480	100	30 to 450	500	*	*	3
Daqing Field, China	Sandstone	3934	328 to 393	20 to 30	50 to 5000	113	9 to 10	500 to 2500	5000 to 7000	0.6	15
La-sa-Xing Filed, China	Sandstone	2011 to 5614	*	17 to 27	2000	117 to 128	8 to 10	*	5000 to 7000	*	10
North Stanley Stringer, Oklahoma	Sandstone	2900	*	18	300	105	2.2	100 to 600	*	.024 to .07	3.1
West Selmek. Crook County. WY	Sandstone	7240	27	20	647	144	12.3	200	7750	0.15	4.4
Taber Maniville south	Sandstone	3230	*	26	2107	95	58	360 to 500	*	0.2	2

Fig. 2.18 – Polymer flooding field case studies outside of Canada (Shehata *et al.* 2012)

Published literatures on some of the most successful and unsuccessful polymer flooding field cases around the world can be summarized as follows:

- Most commonly used polymers are the polyacrylamides. They are widely used mainly because of their low cost compared to other EOR polymers.
- Polyacrylamides are used in reservoirs with salinity ranging from 700 to 25000 ppm.
- Reservoirs with salinity content of more than 30,000 ppm are not suitable for polymer flooding (Shehata *et al.* 2012).

- Screening criteria suggested by many authors indicate that polymer flooding can be applied in reservoirs with oil viscosities between 10 cp and 150 cp (Seright, 2010). However, the highest oil viscosity in which success has been achieved until 2004 was 126 cp (Du and Guan, 2004).
- For reservoirs having oil viscosities above 150 cp, polymer flooding processes have failed mainly because of injectivity problems. The polymer viscosity requirements to achieve a favorable mobility ratio would reduce the solution injectivity to prohibitively low values causing the oil production rate to become uneconomically low.
- Polymer flooding undertaken in reservoirs extensively flooded by other processes (including water flooding) have been largely unsuccessful. Much success can be achieved when polymer flooding is applied to reservoirs at earlier stages of secondary recovery.
- Conclusions from previous studies indicate that polymer flooding carried out with polymer slug sizes smaller than 7% PV have not been successful (Du and Guan, 2004).

CHAPTER 3

POLYMER SOLUTION PREPARATION AND RHEOLOGICAL CHARACTERIZATION

3.1 Polymer Molecular Weight and Solution Concentration

Choosing the right molecular weight (M_w) of polymer for a given polymer flood project is very important as it significantly affects the effectiveness of the project. Polymer molecular weight is selected such that, it is high enough to provide greater viscosity for better mobility control but at the same time small enough so that polymer can enter and propagate effectively through the pore throats of the reservoir rocks and minimize injectivity problem (Zhang *et al.* 2004). To avoid pore blocking by polymer molecules, lower molecular weight polymers are used in case of reservoirs with low permeability.

Another way of choosing polymers is based on their molecular weight distribution. When polymers with wider MWD flow through porous media, because of the diverse hydrodynamic radii of polymer molecules, they can enter and propagate through different pore-throat sizes more effectively and reduce the volume of inaccessible pores; consequently displacing oil more efficiently (Wang *et al.* 2009).

Quite similar to choosing the right molecular weight, the polymer concentration must be selected such that a balance between achieving higher viscosity and minimizing injectivity problem is maintained. It is found that, the effectiveness of flooding can be increased by injecting polymer solution with higher

concentration during the initial stages of polymer flooding. During the final stages, the increase in water-cut can be minimized by again increasing the concentration of polymer solution (Yang *et al.* 2004; Wang *et al.* 2009).

3.2 Polymer Solution Preparation

3.2.1 Polymers Used

HPAM grades listed in **Table 3.1** were supplied by SNF S.A.S in odor-free, white granular powder form with molecular weights ranging from 0.5×10^6 Dalton to 20×10^6 Dalton. These polymers are anionic, water-soluble with a degree of hydrolysis of 25-30 mole %.

Polymer solutions were prepared in such a way that they all exhibit identical shear viscosity behavior but different elastic properties. By keeping the average molecular weight constant and varying the molecular weight distribution (MWD), it was possible to prepare HPAM solutions with identical shear viscosity but different elasticity.

Table 3.1 – HPAM grades and their average molecular weights	
HPAM Grade	Average Molecular Weight (M_w)
3630 S	20,000,000
3330 S	8,000,000
3130 S	2,000,000
AB 005V	500,000

3.2.2 Polymer Solution Composition

By keeping the same average molecular weight but different molecular weight distribution (MWD), it was possible to prepare polymer solutions with constant shear viscosity and variable elastic characteristics. MWD depends on polydispersity index, I which is given by the following equation (Zang *et al.* 1987),

$$I = \frac{M_w}{M_n} = \left(\sum_{i=1}^n \omega_i M_{w,i} \right) \left(\sum_{i=1}^n \frac{\omega_i}{M_{n,i}} \right) \quad (3.1)$$

Where, M_w is weight average molecular weight, M_n is the number average molecular weight and ω_i is the weight fraction of polymer grade i .

The average molecular weight of polymer blend is given by the equation,

$$M_{w,B} = \sum_{i=1}^n \omega_i M_{w,i} \quad (3.2)$$

Even though polydispersity index cannot be used as an absolute measure of MWD, it is true without an exception that, higher polydispersity index indicates wider MWD. Statistical explanation given by Sheu in 2001 states that, polydispersity index is a good measure of the width of molecular weight distribution of polymers.

Due to the unavailability of Mn data for the polymer grades used, polydispersity index of polymer solutions were not calculated. Instead, the elastic nature of these solutions was quantified using their elastic modulus.

Weight fractions of polymer grades were adjusted in such a way that the average molecular weights of the blends were close to 2×10^6 Dalton and 8×10^6 Dalton. Polymer solution concentration was kept constant at 0.1 wt%. **Table 3.2** shows the composition and weight average molecular weights of all HPAM samples.

Table 3.2 – Composition and weight average molecular weights of HPAM samples					
HPAM Sample	Mass Fraction of HPAM Grades				Avg. Molecular Weight ($M_{w,B}$)
	3630	3330	3130	AB005	
HPAM 1	0	0	1.0	0	2.000E+06
HPAM 2	0.11	0.15	0.41	0.33	2.008E+06
HPAM 3	0.25	0.00	0.35	0.40	2.043E+06
HPAM 4	0.20	0.16	0.15	0.49	2.006E+06
HPAM 5	0	1.0	0	0	8.000E+06
HPAM 6	0.45	0.25	0.30	0	8.000E+06
HPAM 7	0.59	0.19	0.05	0.17	8.000E+06

As shown in **Table 3.2**, the first four HPAM blends (HPAM-1 to HPAM-4) have the same average molecular weight of 2×10^6 Dalton. Similarly, HPAM-5, HPAM-6 and HPAM-7 were prepared to have the same average molecular weight of 8×10^6 Dalton. The samples with same average molecular weight will have similar shear viscosity; whereas different MWD imply different elastic characteristics of polymer samples.

3.2.3 Procedure for the Preparation of HPAM Solutions

All polymer solutions were prepared by adding calculated quantities of HPAM grades directly to deionized water. Deionized water was produced using the Elga Purelab Ultra shown in **Fig. 3.1**.

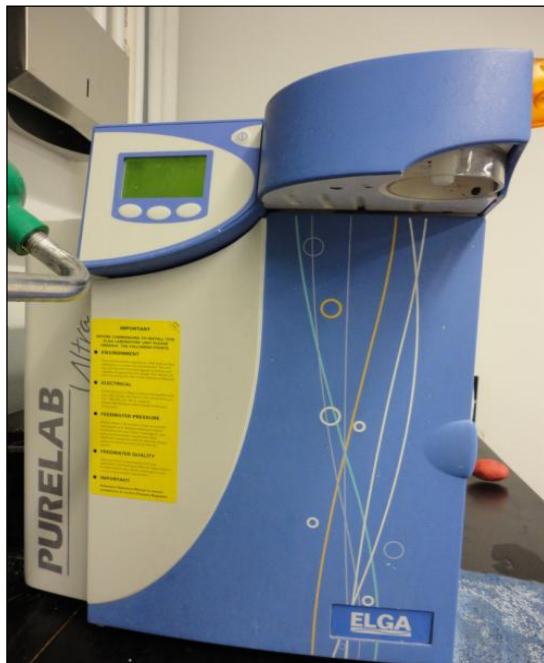


Fig. 3.1 – Elga Purelab Ultra

In order to ensure optimum solution properties, the polymers were mixed in strict accordance with the procedure recommended by the polymer manufacturer.

Separating individual resin particles from each other during the initial stages of stirring is the most important step in dissolving the HPAM polymers; therefore,

vigorous stirring was applied for the initial dispersion of the powder by use of a Hamilton Beach overhead mixer (**Fig. 3.2**).



Fig. 3.2 - Hamilton Beach overhead mixer

This helped to avoid the agglomeration of partially dissolved polymer particles and the formation of gels. Polymers must not be added to water too rapidly in order to avoid lumping of the powder. Adding polymers too slowly would prevent proper dissolution of the powder because of solution thickening before adding the rest of the powder. Also, high-speed agitation of dissolved HPAM solutions was avoided, since the polymers can rapidly degrade at high shear.

HPAM grades were added in the decreasing order of their molecular weights. Powders were added in three lots with constant stirring maintained at 300 to 350

rpm using a magnetic stirrer. The speed of the stirrer can be adjusted to ensure a stable vortex has formed. A Hamilton Beach overhead mixer was used to mix the solution thoroughly after the addition of each lot for about 6 seconds. Finally when all three lots were added, the solution was stirred vigorously for about 15 seconds.

3.3 Rheological Characterization

Two types of rheology tests were conducted in order to characterize HPAM solution; Viscometry test and Oscillation test. A C-VOR 150 Peltier Bohlin rheometer (**Fig. 3.3**) with cone and plate measuring system was used for these tests. Polymer samples were placed in between a stationary plate with a diameter of 60 mm and a rotating upper cone with a 4° angle and a diameter of 40 mm, separated by a gap of 150 µm. All measurements were carried out at laboratory room temperature.



Fig. 3.3 – Bohlin Rheometer

3.3.1 Viscometry Test

The viscometry test studies the viscosity and flow of tested samples as a function of shear, time or temperature. The test consists of the delay and the integration intervals. The shear is applied for the delay time; the average value of shear stress (or shear rate if stress is applied) is measured during the integration time and the viscosity is then calculated.

In this study, flow and viscosity of the polymer solutions were measured at shear rates ranging from 1 to 100 s⁻¹. Since the relationship of shear stress to shear rate is strictly related to the flow, the flow characteristics of the tested samples were

presented by plotting shear stress vs. shear rate. Shear viscosity was also plotted using the viscometry test data.

3.3.2 Oscillation Test

The oscillation test measures viscoelastic properties of materials, which can be studied as a function time, temperature or frequency. There are two types of oscillation tests, 1) amplitude sweep test, and 2) frequency sweep test.

3.3.2.1 Amplitude Sweep

The amplitude sweep test is performed to define the region of linear viscoelastic response (LVR) of tested samples. Materials exhibit linear viscoelastic behavior, when strain and rate of strain are infinitesimal and, therefore, the ratio of stress or strain is independent of the stress magnitude, but is a function of time (or frequency) only.

In the amplitude sweep test, test samples are oscillated at a fixed frequency and slowly increasing amplitude (strain or stress). The measured viscoelasticity values remain constant within the LVR. When the applied stress becomes too great, the induced strain will start to break the elastic structure of tested samples. Thus, strains below that point should be used to work within LVR.

Results of amplitude sweep tests are used for subsequent tests, i.e. the LVR region is determined and a stress value falling within the LVR is selected, which is consequently used in other rheological tests.

3.3.2.2 Frequency Sweep

The frequency sweep test measures viscoelastic properties of tested materials as a function of frequency. During the test, a varying frequency is applied on tested samples with a constant value of stress. The test consists of the delay and sampling intervals: frequency is applied during the delay time and the phase shift δ between the stress and the strain as well as the complex modulus G^* is measured during the sampling interval. Other viscoelastic functions, including the elastic modulus G' and the viscous modulus G'' , are then calculated.

The complex modulus is obtained from the ratio of the stress amplitude to the strain amplitude. It is the sum of the elastic component G' and the viscous component G'' .

The complex modulus is given by:

$$G^* = G' + i \times G'' \quad (3.3)$$

The elastic modulus G' is usually referred to as the storage modulus to describe the elastic storage of energy, because strain is recoverable in elastic materials.

The viscous modulus G'' is referred to as loss modulus to describe the viscous dissipation or loss of energy due to permanent deformation in flow.

The parameter G' and G'' are given as (Shaw and MacKnight, 2005):

$$G' = G^* \cos\delta \quad (3.4)$$

$$G'' = G^* \sin\delta \quad (3.5)$$

Oscillation tests provide important information related to the viscoelasticity of polymer solutions. Through these tests, one can determine whether viscous nature or the elastic nature of polymer is dominating over a given range of shear or angular frequency.

Fig. 3.4 shows the viscous modulus and elastic modulus of HPAM-4 and the cross-over point.

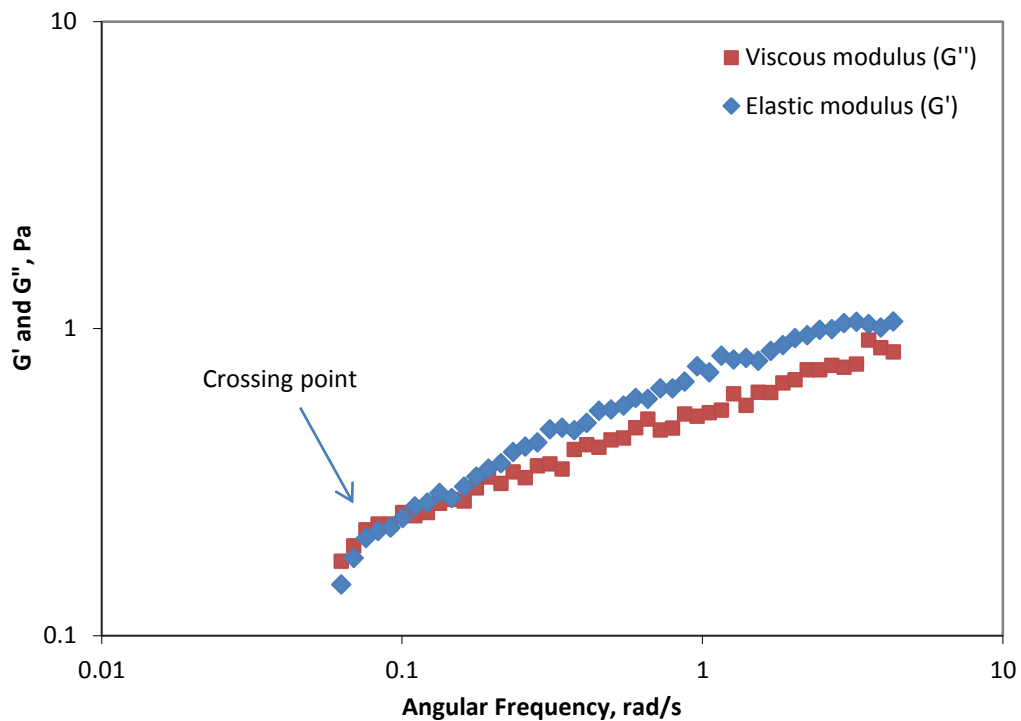


Fig. 3.4 – G' and G'' vs Angular Frequency for HPAM-4

It is found from the literature that the storage modulus, G' and the loss modulus, G'' increase with polymer concentration and viscoelasticity becomes more and more prominent. When G' and G'' are plotted against angular frequency, there exists a cross-over point where the corresponding frequency is called the specified frequency (SF). As the concentration of HPAM increases, the SF

moves to lower frequency. When the angular frequency is less than ω_c , G'' is more than G' , i.e. viscous effect is dominating. When the angular frequency is more than ω_c , G' is greater than G'' which implies that the elastic effect is more dominating (Meng *et al.* 2008).

CHAPTER 4

CORE FLOODING EXPERIMENTS

4.1 Materials Used

4.1.1 Polymers

Seven different HPAM solutions with two different average molecular weights and a range of MWD were used for radial core flooding experiments. Their composition and weight average molecular weights given in **Table 3.2**. Preparation of HPAM solutions has been explained in the previous chapter.

The first four HPAM blends (HPAM-1 to HPAM-4) have the same average molecular weight of 2×10^6 Dalton. Their elastic modulus varied such that HPAM-1 had the lowest elasticity followed by HPAM-2 and HPAM-3 with HPAM-4 having the highest elasticity. Similarly, HPAM-5, HPAM-6 and HPAM-7 were prepared to have the same average molecular weight of 8×10^6 Dalton but variable elasticity (**Table 3.2**).

4.1.2 Mineral Oil

Light mineral oil used in the experiments had the physical properties as given in **Table 4.1**. It is composed mainly of paraffins and cyclic paraffins.

Table 4.1 – Physical properties of mineral oil (Fisher Scientific® Product Data Sheet)	
Property	Description
Physical state	Liquid
Appearance	Water-white
Odour	None
Vapour Pressure	< 0.1 mm Hg
Viscosity	< 33.5 centistokes @ 40°C
Boiling Point	260-426°C
Solubility	Insoluble in water
Specific Gravity/Density	0.83@15.6°C
Molecular Composition	Paraffin mixture
API Gravity	39° API

4.1.3 Porous Media

Potters Industries Inc. supplied SPHERIGLASS A-GLASS 3000 grade glass beads were used as porous media in all flooding experiments. Glass beads had a particle size distribution of 30-50 microns and a specific gravity of 2.5. The absolute permeability of the porous medium was found to be 150 mD.

4.2 Experimental Setup

The main components of the experimental setup include 1) a radial core holder designed to simulate radial flow, 2) a constant rate LC-5000 syringe pump for

injecting oil and polymer, 3) a pressure transducer for pressure measurements and a data logger for recording pressure data digitally on a computer, and 4) graduated measuring jars for collecting and measuring effluents. A schematic of the experimental set-up is shown in **Fig. 4.1**.

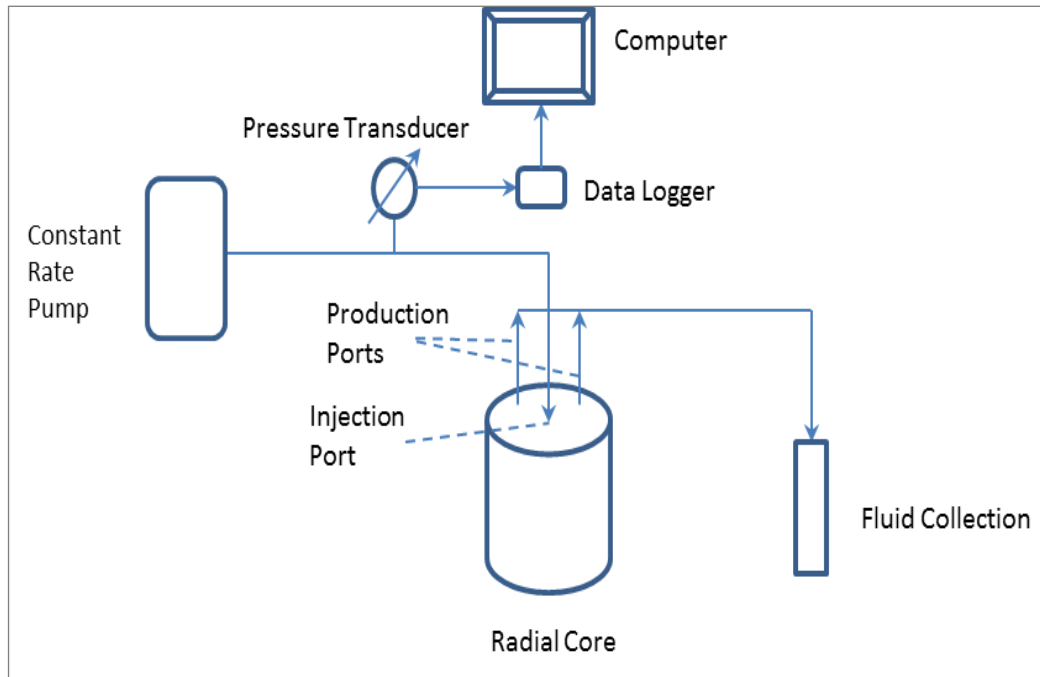


Fig. 4.1 – Schematic of the radial core flooding setup

4.2.1 Radial Core Holder

Flooding experiments were conducted in a radial core holder designed to simulate radial flow. The core holder had an internal diameter of 98 mm and a height of 191 mm. It had one injection well located at the center and two production wells at the periphery. The lower 145 mm section of the injection well was perforated. Injection line had a radius of 7 mm and both production lines had a radius of 3.6 mm. Injector and producers were tightly wounded by a

screen with 10 micron opening. Actual photograph of the radial core holder is shown in **Fig. 4.2**.



Fig. 4.2 – Radial Core Holder

4.2.2 Syringe Pump

A constant flow rate ISCO LC-5000 syringe pump was used for saturating the core holder with mineral oil and then for polymer flooding. The pump with a maximum pressure of 3700 psi (25.5MPa) has a 500-ml capacity and flow rate range of 0.1 ml/hr up to 400 ml/hr.

The picture of the syringe pump used for radial core flooding experiments is shown in **Fig. 4.3**.



Fig. 4.3 – Constant Rate Syringe Pump

4.2.3 Data Acquisition System

The data acquisition system used was made up of two pressure transducers connected to the data logging system. These two pressure transducers had different pressure ranges of 0-100 psi and 0-500 psi and were supplied by Omega dyne. A National Instruments data acquisition system (NI USB-9219) was used which transferred the pressure readings to the computer. These pressure readings were then interpreted and recorded using the Labview Signal Express software, also supplied by National Instruments.

4.3 Experimental Procedure

4.3.1 Procedure for Packing the Core Holder

The core holder was packed with SPHERIGLASS A-GLASS 3000 grade dry spherical glass beads with the help of a mechanical vibrator operated by air pressure. The mechanical vibrator was pressed onto the cell walls while dry glass beads were poured into the core holder. Vibration continued until the entire granular material dispersed evenly and packed closely in the core holder. When no more glass beads could be loaded, the loading was stopped and the core holder was secured properly. Core holder is now ready to be saturated with mineral oil.

4.3.2 Porosity Measurement

The pore volume of the porous medium was measured using the direct method by subtracting the volume of glass beads in the core holder from the bulk volume, i.e. the total volume of the core holder. Therefore, the weight of the glass beads loaded into the core holder was recorded and the volume of the material was determined accurately for each experiment. A specific gravity of 2.5 as specified by the glass beads manufacturer was used in the calculations.

4.3.3 Permeability Measurements

Permeability measurement experiments conducted by Urbissinova in 2010 are explained below. Water was injected at different flow rates into the core holder initially packed with glass beads and corresponding pressure drops were

measured. Stabilized pressure drop data obtained for different water flow rates were plotted as shown in **Fig. 4.4**.

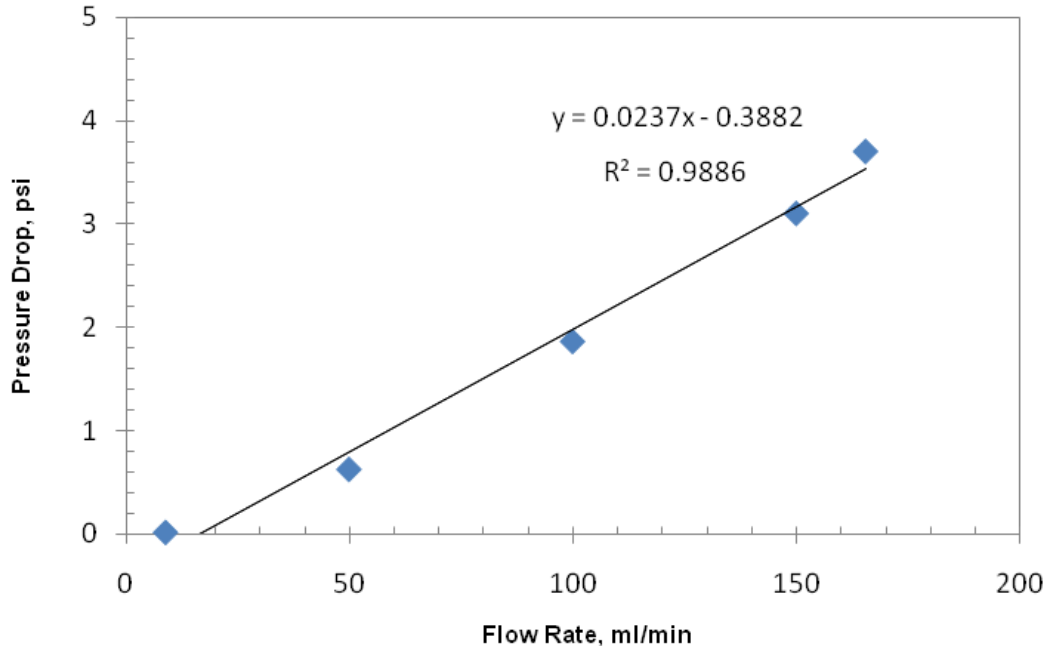


Fig. 4.4 – Pressure drop – Flow rate profile for water injection

The absolute permeability of the porous medium was calculated using Darcy's law for radial steady-state flow given by **Eq. 4.1**,

$$Q = \frac{2\pi kh(P_e - P_w)}{\mu \cdot \ln\left(\frac{r_e}{r_w}\right)} \quad (4.1)$$

Where,

Q is flow rate, ml/min

k is the absolute permeability of the porous medium, Darcy

h is height of the core, cm

P_e is the pressure at the external boundary, psi

P_w is pressure at the wellbore, psi

μ is the dynamic viscosity of water, Pa.s

r_e is the radius at the external boundary, cm

r_w is the radius of the wellbore, cm

Using the slope of the pressure profile shown in **Fig. 4.4**, the absolute permeability of the porous medium was calculated as follows,

$$k = \frac{\mu}{2\pi hm} \ln\left(\frac{r_w}{r_e}\right) = \frac{0.00089 \text{ Pa.s} * \ln\frac{0.69 \text{ cm}}{4.9 \text{ cm}}}{2 * 3.142 * 19.1 \text{ cm} * 0.0237 \frac{\text{psi}}{\text{ml/min}}} = 150 \text{ mD} \quad (4.2)$$

4.3.4 Shear Rate Determination

Christopher and Middleman (1965) suggested a relationship (**Eq. 4.2**) that could be used to estimate shear rates applicable for the flow of power law type fluids through porous media;

$$\gamma = \frac{3n + 1}{4n} \cdot \frac{4Q}{A(8k\Phi)^{0.5}} \quad (4.2)$$

Where γ is shear rate, 1/s, $3n + 1 / 4n$ is a non-Newtonian correction factor for power-law fluids with n being the flow behavior index, Q is flow rate, cm^3/s , A is cross sectional area of the core, cm^2 , k is permeability, cm^2 , and Φ is porosity.

At very low flow rates power law constant, n can be omitted without any serious loss of accuracy. Since the core holder has a radial geometry, the cross sectional area term in the **Eq. 4.2** will vary and as a result the fluid will undergo variable shear rates as it flows from the center to the periphery. A constant flow rate of 4 ml/min was used throughout the core flooding experiments. Using the power law coefficients shown in **Table 5.1**, correspondingly, the fluid will be exposed to a range of shear rates between 10 1/s and 100 1/s. This is within the range of shear rates typically observed in water flooding operations in the field (Jennings *et al.* 1971; Gleasure and Phillips, 1990; RP 63, 1990).

4.3.5 Flooding Procedure

After the core holder was packed with glass beads, it was saturated with mineral oil. The volume of oil required to saturate the core holder, which depends on the pore volume, was recorded. Pore volume of the porous medium was determined using direct method by subtracting the volume of glass beads in the core holder from the bulk volume of the core holder.

Flooding experiments were then started with polymer solutions prepared as per the procedure explained earlier. Polymer was pumped at a constant flow rate of 4 ml/min using a syringe pump. Pressure was monitored throughout the experiment using a pressure transducer and pressure readings were recorded on to a computer using a data logger.

Effluents (oil + polymer) produced were collected at regular intervals and the volume of oil and polymer collected were measured separately. The produced polymer samples were also analyzed for any changes in viscosity and elastic properties. Flooding was continued until either the volume of oil produced was too low or the water cut was greater than 90%. Typically the volume of polymer injected was around ~1.9 PV.

CHAPTER 5

**CORE FLOODING EXPERIMENTS: RESULTS AND
DISCUSSION**

In this chapter, the rheological test results of HPAM solutions used for core flooding experiments are discussed. Also, detailed analyses of core flooding experimental results are given.

5.1 Rheological Characterization of HPAM Solutions

Two types of rheology tests were conducted: viscometry tests and oscillation tests.

5.1.1 Viscometry Tests

The viscometry tests studied the shear viscosity and flow of the HPAM solutions as a function of shear. The viscosity behavior was measured at shear rates from 1 to 100 1/s. Shear stress vs. shear rate profiles for HPAM-1 to HPAM-7 generated using the viscometry test results are shown in **Fig. 5.1**.

As shown in **Fig. 5.1**, the shear stress vs. shear rate profiles of HPAM-1 to HPAM-4 and HPAM-5 to HPAM-7 were identical at a range of shear rates from 1 to 100 1/s.

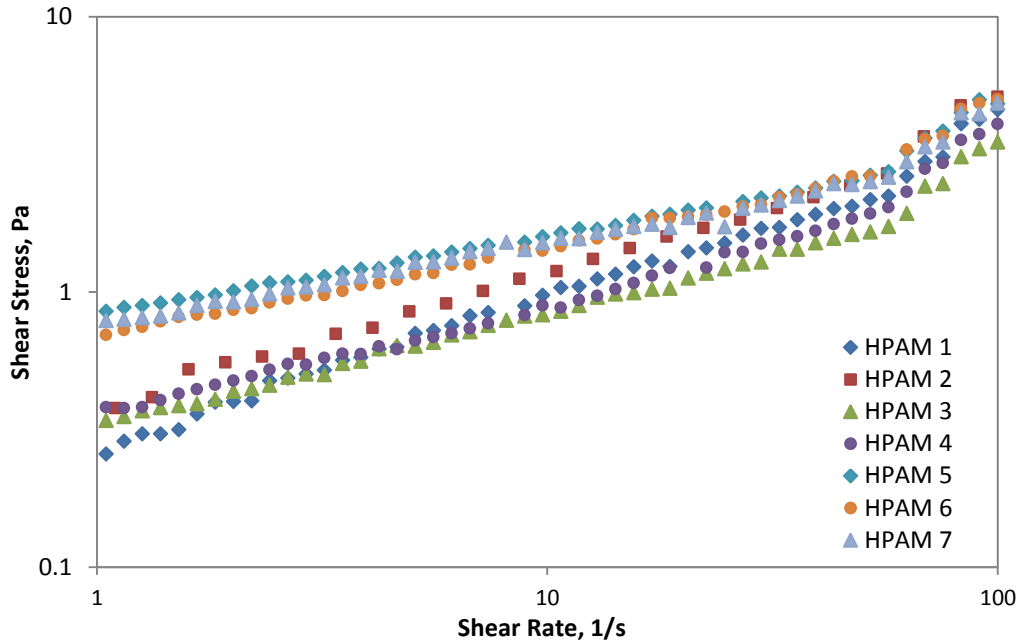


Fig. 5.1 – Shear Stress vs. Shear Rate profiles for HPAM-1 to HPAM-7

Also, the shear stress vs. shear rate values of the HPAM solutions shown in the figure indicate that the rheological behavior of the samples can be characterized by the power-law model within the covered range of shear rates.

Table 5.1 - Power law parameters of HPAM samples		
HPAM Samples	K, Pa.s ⁿ	n
HPAM 1	0.2665	0.5614
HPAM 2	0.3594	0.5264
HPAM 3	0.3059	0.4567
HPAM 4	0.3222	0.4736

The consistency index, K , and power law index, n , for HPAM samples obtained from **Fig. 5.1** are listed in **Table 5.1**. From **Fig. 5.1**, it can be concluded that HPAM samples follow power law model. K is a constant, which is equivalent to Newtonian viscosity as n approaches to 1. Very close values of K indicate that, all four HPAM solutions have similar viscosity behavior, which can be explained by almost identical values of average molecular weights of HPAM samples as shown in **Table 3.2**.

Fig. 5.2 shows the shear viscosity behavior of all seven HPAM samples as a function of shear rate. Shear viscosity values of HPAM solutions having the same average molecular weight were found to be lying very close to each other. HPAM samples 1 to 4 having an average molecular weight of 2×10^6 Dalton show shear viscosity values lower than the HPAM samples 5 to 7 having an average molecular weight of 8×10^6 Dalton.

All these polymer samples showed an increase in shear viscosity beyond a particular shear rate (sometimes referred to as critical shear rate). This behavior is known as shear-thickening and can be interpreted as due to the elastic stretching of polymer molecules, which has been studied in detail by several authors (de Gennes, 1974; Hirasaki and Pope, 1974; Haas and Durst, 1981; Magueur and Moan, 1985; Odell and Keller, 1986; Ait-Kadi et al. 1987; Dupuis et al. 1994; Hu et al. 1994).

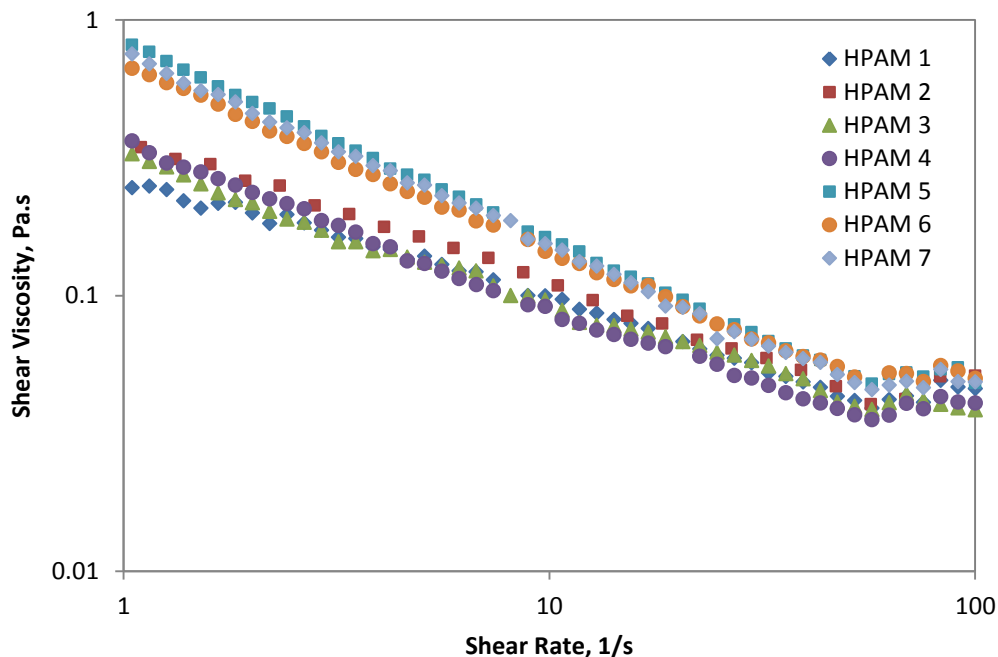


Fig. 5.2 – Shear Viscosity vs. Shear Rate profiles for HPAM-1 to HPAM-7

5.1.2 Oscillation Tests

Oscillations tests involve measuring viscous and elastic modulus of polymer solutions as a function of either shear stress (amplitude sweep test) or angular frequency (frequency sweep test).

In this study, frequency tests were conducted on HPAM samples at a range of frequency from 0.01 Hz to 1 Hz, while the shear stress was kept constant at 0.04755 Pa. The viscous modulus and elastic modulus were plotted against angular frequency and analyzed.

As shown in **Fig. 5.3**, the viscous moduli of HPAM samples 2, 3 and 4 are very close to each other through the frequency range of 0.1 to 10 rad/s. Viscous modulus of HPAM-1 is slightly lower than the other HPAM samples in the low

angular frequency region. However, at angular frequency between 0.5 to 5 rad/s, they all have similar viscous moduli. HPAM-5 to HPAM-7 samples with an average molecular weight 8×10^6 Dalton have identical viscous modulus but greater than that of HPAM-1 to HPAM-4 samples with an average molecular weight 2×10^6 Dalton.

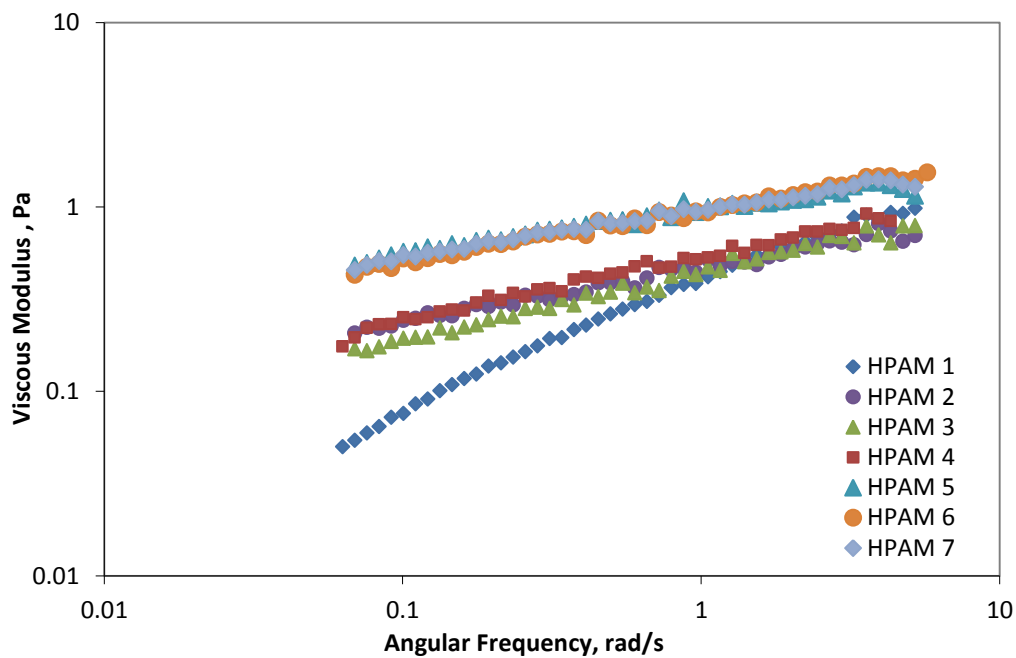


Fig. 5.3 – Viscous Modulus vs. Angular Frequency for HPAM-1 to HPAM-7

Results from **Fig. 5.2** and **Fig. 5.3** imply that, HPAM samples with higher average molecular weight will have higher shear viscosity or viscous modulus.

Fig. 5.4 shows the elastic modulus of all HPAM samples plotted against angular frequency.

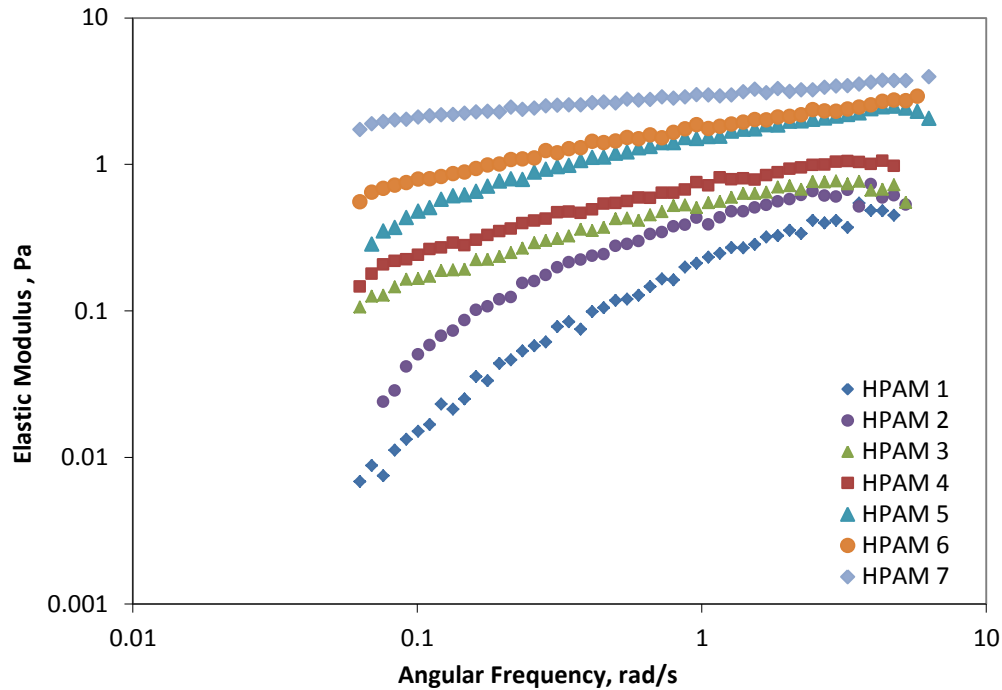


Fig. 5.4 – Elastic Modulus vs. Angular Frequency for HPAM-1 to HPAM-7

The elastic modulus vs. angular frequency graph (**Fig. 5.4**) indicates that among polymers having the average molecular weight 2×10^6 Dalton, HPAM-4 has the highest elasticity followed by HPAM-3, HPAM-2 and HPAM-1. Close values of elasticity of HPAM-3 and HPAM-4 indicates that they have similar MWD widths. Among polymers having the average molecular weight 8×10^6 Dalton, HPAM-7 has the highest elasticity followed by HPAM-6 and HPAM-5.

5.2 Core Flooding Experimental Results

Seven HPAM samples having two different average molecular weights and variable elasticity values were flooded into the radial core saturated with mineral oil to study the effect of elasticity on recovery efficiency.

5.2.1 Pressure Drop during Flooding Experiments

Pressure readings recorded during the flooding experiments are presented in **Fig.**

5.5.

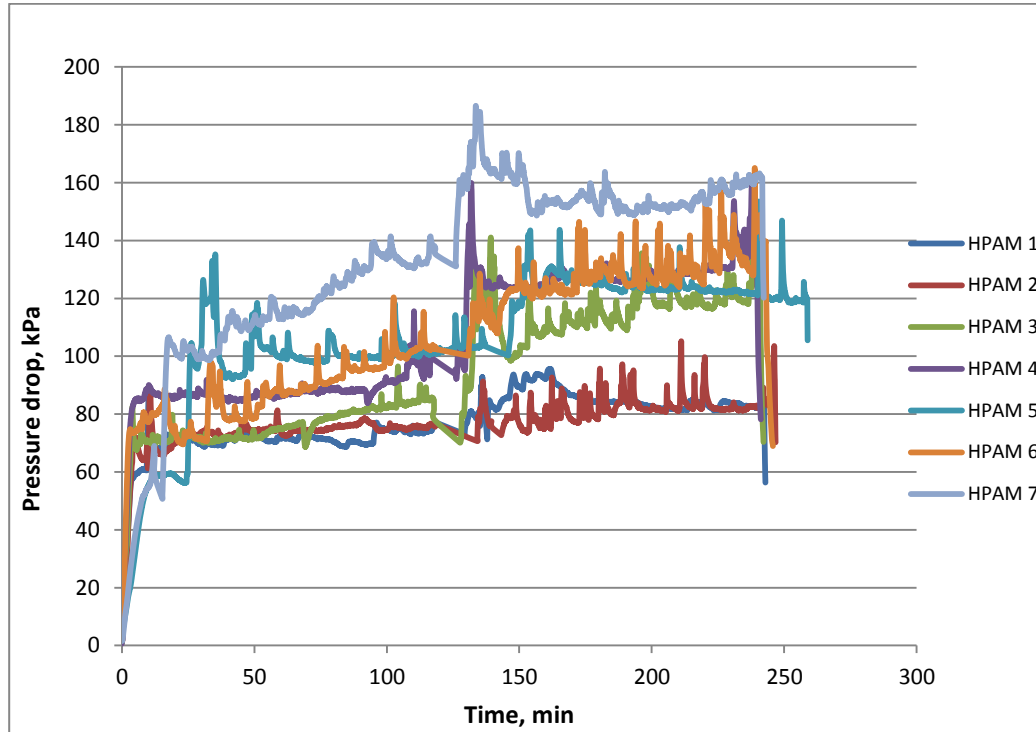


Fig. 5.5 – Pressure Drop during Polymer Flooding Experiments

Polymer samples with higher viscosity and/or elasticity witnessed greater pressure drops than the ones with lower viscosity and/or elasticity values. Higher pressure drops indicate that there is greater resistance to flow due to higher elasticity of polymer samples, which supported the results from rheology measurements. However, these pressure plots did not provide any information on the breakthrough points during the flooding process.

5.2.2 Oil Recovery Performance and Polymer Elasticity

The variation of cumulative oil recovery as a function of volume of polymer solution injected is shown in **Fig. 5.6**. Of all the polymers with an average molecular weight of 2×10^6 Dalton, HPAM-4, which has the highest elasticity resulted in the highest oil recovery of 75.2% while, HPAM-1, which has the lowest elasticity, resulted in the lowest oil recovery of 64.7%. The elastic modulus of HPAM-4 is 16 times greater than that of HPAM-1 at an angular frequency of 0.1 rad/s and 3 times at an angular frequency of 1 rad/s.

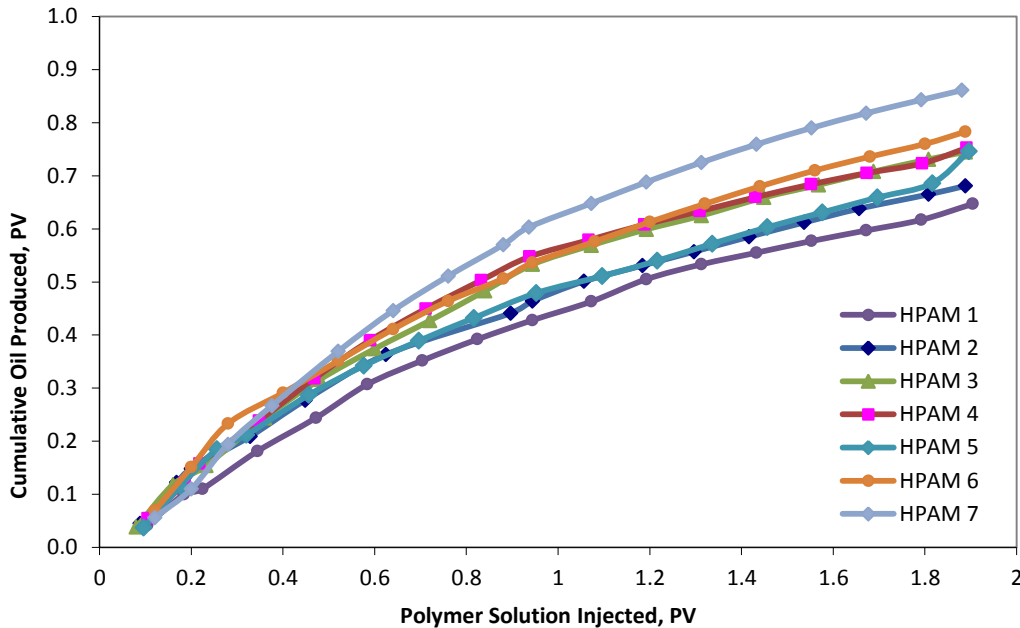


Fig. 5.6 – Cumulative Oil Produced vs. Pore Volume of Polymer Injected

Fig 5.7 and **Table 5.2** summarize the results of the influence of MWD (polydispersity index) and average molecular weight on breakthrough and cumulative oil recovery. The recovery performance of these four polymer

samples is in the ascending order of HPAM-1 > HPAM-2 > HPAM-3 > HPAM-4. For all these four polymers, HPAM-1 to HPAM-4, shear viscosity and hence the viscous modulus values are similar within the range of shear rate application as shown earlier in **Fig 5.2** and **Fig 5.3**. Hence, the reason for difference in higher ultimate recovery, ~10%, between HPAM-4 and HPAM-1 polymer solution injection could be mostly due to their elasticity difference. Elastic modulus trend as shown in **Fig 5.4** is also in the ascending order of HPAM-1 > HPAM-2 > HPAM-3 > HPAM-4, and correlates well with the trend in oil recovery.

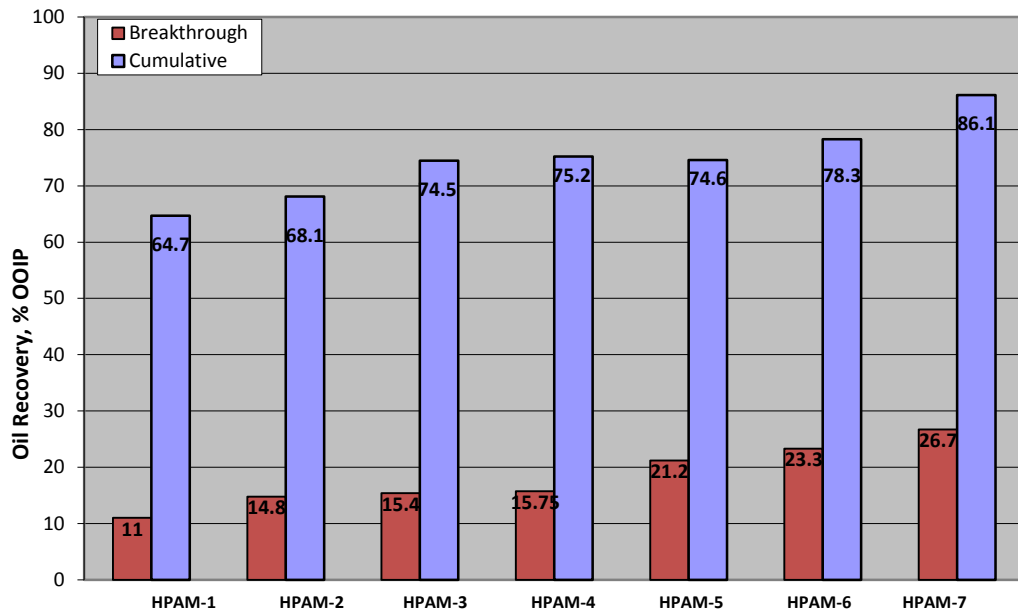


Fig. 5.7 – Breakthrough and Overall Oil Recovery

Table 5.2 – Breakthrough and Overall Oil Recovery		
Polymer Sample	% Recovery	
	at Breakthrough	Cumulative
HPAM 1	11.0	64.7
HPAM 2	14.8	68.1
HPAM 3	15.4	74.5
HPAM 4	15.75	75.2
HPAM 5	21.2	74.6
HPAM 6	23.3	78.3
HPAM 7	26.7	86.1

Results from recovery experiments using low average molecular weight (2×10^6 Dalton) polymer solutions support the idea that, polydispersity index – a measure of elasticity – can be used to screen a polymer among available same average molecular weight polymers for better EOR performance. In order to confirm this conclusion further, we performed similar experiments using HPAM solutions of high molecular weight (8×10^6 Dalton). Among the three polymers with an average molecular weight of 8×10^6 Dalton, HPAM-7 and HPAM-5 resulted in highest and lowest oil recoveries respectively. The ultimate recovery for HPAM-5 polymer injection was 74.6% and that of HPAM-7 was 86.1%. The ~11% higher recovery in case of HPAM-7 correlated well with the fact that HPAM-7 had higher elastic modulus than HPAM-5. The elastic modulus of HPAM-7 is 4.5 times greater than that of HPAM-5 at angular frequency of 0.1 rad/s and 2 times higher at an angular frequency of 1 rad/s.

The difference in oil recovery performance of HPAM-3 and HPAM-4 is very minimal in terms of breakthrough recovery as well as final recovery (**Fig 5.7**). This can be attributed to lower elasticity difference as shown in **Fig 5.4** which indicates small difference in MWD widths. Therefore, along with the previous observation of an increase in elastic modulus resulting in higher breakthrough and final recoveries (HPAM-1 to HPAM-4 and HPAM-5 to HPAM-7), one can say that there exists an optimal MWD (polydispersity index) beyond which the recovery is not significantly affected by the increase in elastic properties.

The results presented in **Fig 5.6** and **Fig 5.7** suggests that both average molecular weight and molecular weight distribution of polymers could affect the recovery performance of polymer solutions. Now, the real question is whether the average molecular weight or the molecular weight distribution has more control on the recovery efficiency.

Conventional polymer flooding field approach assumes that viscoelastic polymers with highest average molecular weight are expected to give better recovery performance. The difference in ultimate recovery between HPAM-5 and HPAM-1 is ~10%, whereas HPAM-5 has four times higher average molecular weight than HPAM-1. It was interesting to see that all three HPAM polymer samples with average molecular weight 8×10^6 Dalton resulted in significantly higher breakthrough recoveries than the ones with average molecular weight 2×10^6 Dalton. The difference in ultimate recovery between

HPAM-7 and HPAM-1 is more than 20%, due to the difference in average molecular weight between two polymer samples of four times and difference in elastic modulus of nearly 140 times at an angular frequency of 0.1 rad/s and 13 times at an angular frequency of 1.0 rad/s.

However, if the average molecular weight is the only criteria for a polymer to perform better during EOR application, HPAM-5 should have performed better than HPAM-4. But, the final recovery of HPAM-5 polymer injection was not significantly different from that of HPAM-4 despite the fact that HPAM-5 polymer solution has higher average molecular weight (8×10^6 Dalton) than HPAM-4 (2×10^6 Dalton).

5.2.3 Amount of Polymer Required

A critical parameter defining the economic success of a polymer flooding operation could be the amount of polymer injected for the amount of oil produced. The amount of polymer required to produce a fixed pore volume of oil is also correlated well with the elasticity of polymer solution. As shown in **Fig 5.6**, when we compare the amount of oil produced after a given pore volume of polymer has been injected, the polymer with higher elasticity has produced more oil compared to the one with lower elasticity. Hence, it can be concluded that, higher the elasticity of HPAM sample, the lower the volume of HPAM solution needed to be injected to produce a fixed volume of oil.

5.3 Changes in Rheological Characteristics of Polymer Solutions before and After Flooding

During the course of flooding, polymer may undergo a considerable amount of shear/mechanical degradation as well as deposition along the porous media which can alter the rheological characteristics of polymer solution. Significant reduction in viscosity may cause lower effective recovery towards the later stages of flooding. The study of the rheological properties of the effluent samples could provide useful information on the degree of polymer viscosity and/or elasticity reduction and its resultant effect on oil recovery efficiency.

In this study, changes in polymer solution rheological characteristics as a result of flow through porous media were assessed by comparing solution viscosities (**Fig 5.8**), solution viscous moduli (**Fig 5.9**), and solution elastic moduli (**Fig 5.10**) of polymer samples injected and produced polymer collected during flooding experiments. All these comparisons have been made between polymers having same average molecular weights i.e., between HPAM-1 and HPAM-4 (average molecular weight 2×10^6 Dalton) and HPAM-5 and HPAM-7 (average molecular weight 8×10^6 Dalton). The concentration of polymer (effluent) after the flooding experiment was not measured, and therefore, it is not known clearly how much of the change in polymer solution rheological characteristics were due to shear/mechanical degradation or deposition along the porous media.

HPAM solution's viscous nature dominates at low flux where as its elastic nature dominates at higher fluxes (Seright, 1980). The flux was kept constant in

all experiments in order to distinguish the elastic and viscous properties in terms of average molecular weight and molecular weight distribution.

From **Fig 5.8**, it can be concluded that HPAM-1 and HPAM-5 have undergone more viscosity reduction than HPAM-4 and HPAM-7 respectively. High degree of viscosity reduction could also be one of the reasons why HPAM-1 and HPAM-5 gave lower oil recoveries than HPAM-4 and HPAM-7 respectively.

Fig 5.9 further supports the above conclusions as they compare viscous modulus reduction during polymer flooding. When elastic moduli were compared (**Fig 5.10**), it was observed that higher elasticity HPAM samples underwent a change to a lesser extent than the ones with lower elasticity and thus resulting in higher oil recovery.

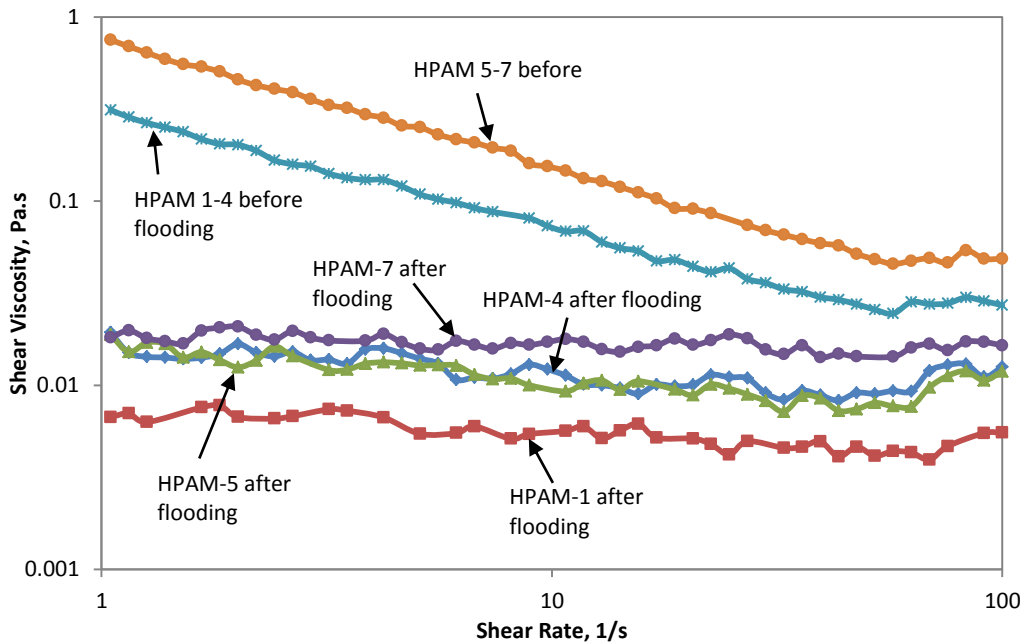


Fig 5.8 – Shear Viscosity Reduction Plots

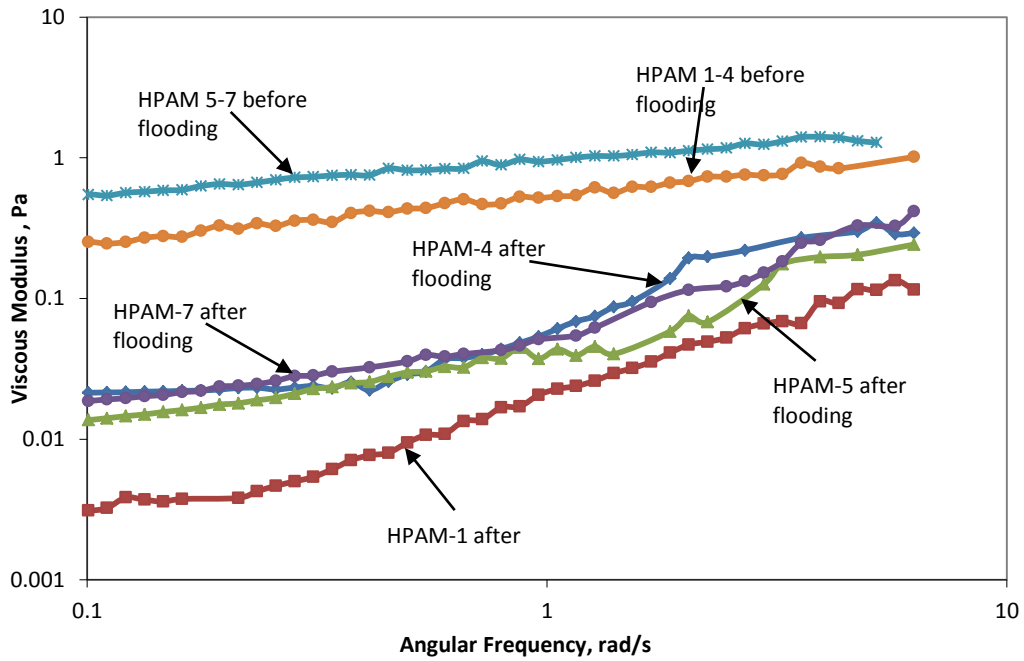


Fig 5.9 – Viscous Modulus Reduction Plots

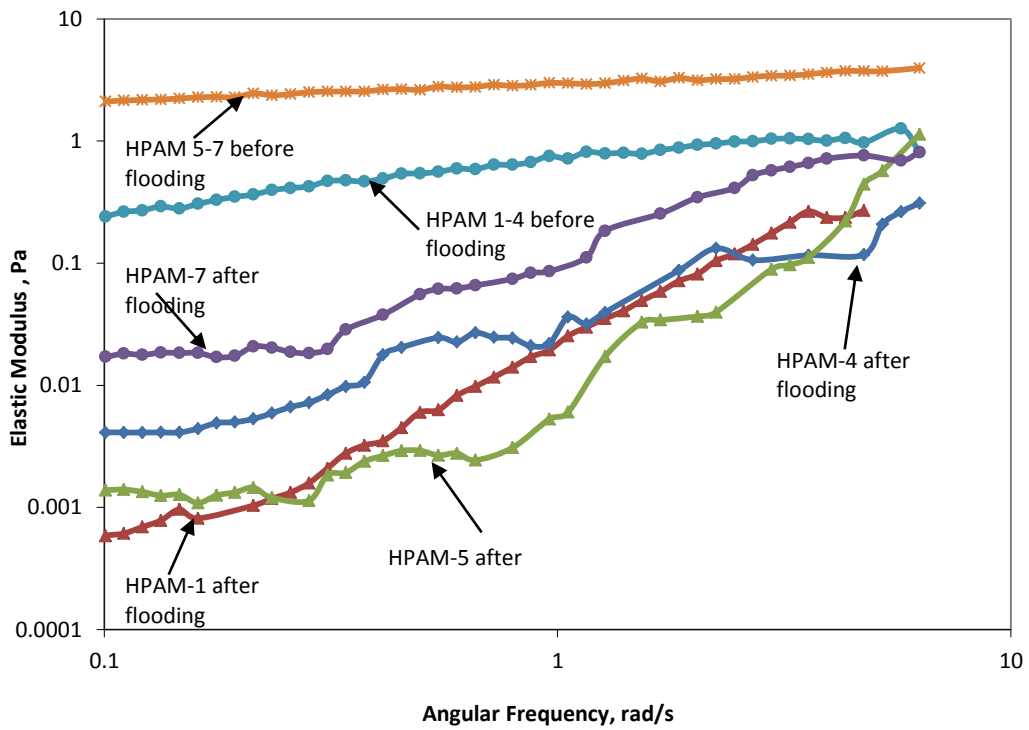


Fig 5.10 – Elastic Modulus Reduction Plots

CHAPTER 6

VISUALIZATION EXPERIMENTS

6.1 Overview

Viscoelasticity of polymers is known to contribute significantly towards improved displacement efficiency in polymer flood operations. But the contribution of elasticity of viscoelastic polymers in enhanced oil recovery (EOR) still remains largely unexplored. Majority of literature available on polymer aided EOR, in general, talks about the role played by viscoelasticity of polymers on improved oil recovery with little or no mention of the individual contribution of elasticity of polymers on EOR.

In this work, partially hydrolyzed polyacrylamide (HPAM) solutions, having identical shear viscosity but different elasticity, were flooded to investigate the individual effect of elasticity on improved oil recovery. A transparent, sand packed visual cell, initially saturated with mineral oil, was used for flooding with four different HPAM solutions. Because these polymer solutions differed only in terms of elasticity, a comparative study of the effect of elasticity on sweep efficiency was done. Photographs taken at regular intervals during the course of flooding were analyzed to study the frontal displacement patterns changing with the elasticity of different HPAM solutions. Mechanism of viscous fingering in immiscible two-phase flow in porous media at different polymer elasticity values was studied.

Laboratory and field experiments have shown that the viscoelastic characteristics of polymer solutions help improve polymer flood efficiency. Through core flooding experiments and numerical simulation, Han *et al.* (1995) concluded that displacement efficiency of a polymer flood operation would reach its maximum when the viscoelastic property of polymer solution is brought into full play. Theoretically, it has also been proved that, the residual oil in sudden expansion pore paths and dead ends that are not recoverable by viscous polymer flooding can be partly displaced when the effect of viscoelasticity is considered. Viscoelastic polymers can partly displace oil trapped in pore throats, in sudden expansion pore paths and in dead ends, thereby increasing the overall oil recovery (Bai *et al.* 2011). Experimental results backed by 1D simulation of polymer flooding performed by Masuda *et al.* (1989) concluded that, the viscoelastic effect of polymer solution plays an important role in the improvement of oil recovery. Work done by Wang *et al.* (2001), Xia *et al.* (2004), Jiang *et al.* (2008) and most recently by Zhang *et al.* (2010) has unanimously suggested that viscoelasticity of polymers improves the displacement efficiency of polymer flood operations. But the individual effect of elasticity of viscoelastic polymers on improved oil recovery remains vaguely understood.

Wang *et al.* (2000) showed that all types of micro-scale residual oil can be reduced after flooding with viscous-elastic polymers. Due to the elastic nature of polymers, the velocity distribution in pores is quite different from Newtonian

fluids and the polymer could also exert a strong “pulling effect” on different types of residual oil. The study pointed out that the relationship between capillary number and the recovery of cores for Newtonian fluids do not apply to fluids with elastic properties. It was also seen that, the increase in micro-scale recovery was related to the increasing elastic properties of polymer fluids. Experiments done by Urbissinova *et al.* (2010) showed that, between the two polyethylene oxide (PEO) blends with identical viscosity behavior and different elastic characteristics, the one with higher elasticity would give higher oil recovery. It was concluded that a more pronounced “expanding piston” behavior induced by the elastic properties of the polymer solutions during the flow in porous media led to higher sweep efficiency and lower residual oil saturation. Another set of experiments done by the same author using two HPAM solutions, having identical shear viscosity but variable elasticity, showed that the polymer solution with higher elasticity yielded higher oil recovery (Urbissinova, 2010). Radial core experiments done by Veerabhadrapa *et al.* (2011) also reiterated the fact that elasticity is an important screening criterion for selecting polymer solutions. Therefore, when selecting a polymer solution for flooding, its elastic properties must be taken into account.

Most chemical EOR processes involve one fluid displacing another with, more-often-than-not, less viscous fluid displacing the more viscous one. Since less viscous fluid has the greater mobility, instabilities always exist. This inevitably causes viscous fingering to appear along the direction of flow. Majority of

flooding experiments done to date (Chouke et al. 1959, Homsy 1987, Jerauld et al. 1984, Yortsos and Huang 1986, Pavone 1992) have described the mechanism of viscous fingering in horizontal immiscible systems through more common governing factors such as, viscosity ratio, capillary number difference, relative permeability, flow rate, interfacial tension etc. Our discussions are limited to situations in which elasticity plays a major role. This has been achieved by isolating the individual effect of elasticity on oil displacement efficiency through visual observations during flooding. Four HPAM samples having constant viscosity but different degree of elasticity were used in flooding experiments.

6.2 Materials Used

6.2.1 Polymers

Four different HPAM solutions (HPAM-1 to HPAM-4 shown in **Table 3.2**) having the same average molecular weight of 2×10^6 Dalton but with different MWD (polydispersity index) were used in the visualization experiments. Polymer solution formulation and preparation steps are explained in previous chapters.

6.2.2 Mineral Oil

Light mineral oil that was used for radial core flooding experiments was also used for visualization experiments. Physical properties of light mineral oil are given in **Table 4.1**. An inert organic dye was used to color mineral oil in order to distinguish oil from polymer solution during the flooding process.

6.2.3 Porous Media

Glass beads used in visualization experiments were of 50-80 mesh size with a particle size distribution of 177-297 microns. They were supplied by Sil Industrial Minerals.

6.3 Experimental Setup

Main components of the experimental setup consisted of; a transparent cell designed to allow radial flow of fluids for visual study, a Chemyx Nexus 250 ml syringe pump for saturating the visual cell and then to flood polymer solution into the cell, a high resolution digital camera mounted on a tripod for capturing displacement fronts during the flooding process at regular time steps, graduated measuring jars for collecting and measuring effluents. A schematic of the experimental set-up is shown in **Fig. 6.1**.

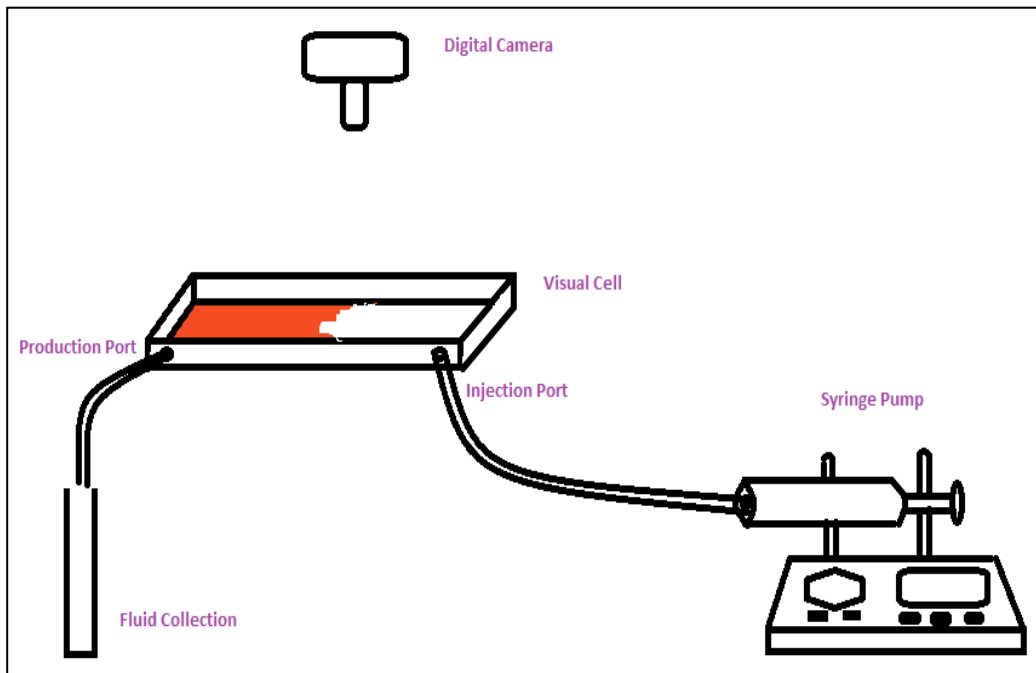


Fig. 6.1 - Schematic representation of the experimental setup

6.3.1 Visual Cell

Horizontal visual cell used for flooding experiments had the dimensions 22.5 cm * 7 cm * 1.4 cm. It was made from acrylic glass material and was kept transparent to allow visual study of displacement patterns. Perforated ports at either ends of the visual cell were used as injector and producer. These ports spanned the entire length of the model. Actual photograph of the visual cell saturated with oil is given in **Fig. 6.2**.

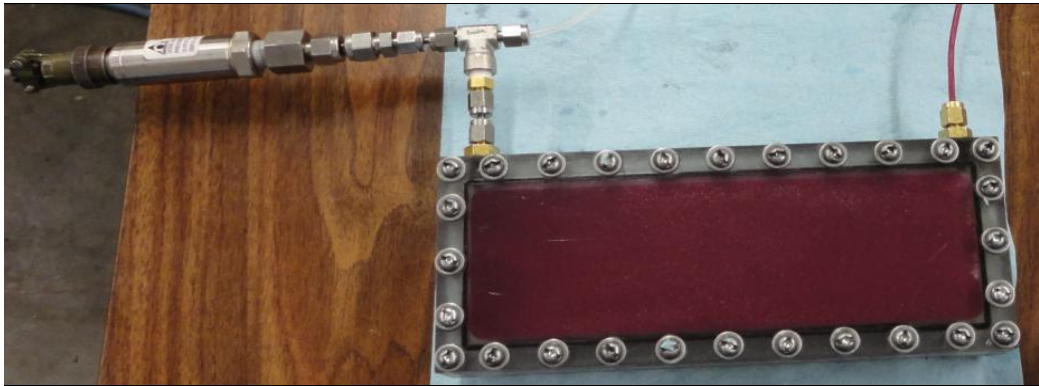


Fig. 6.2 – Visual Cell

6.3.2 Syringe Pump

A Chemyx Nexus syringe pump was used for saturating the visual cell and then to flood polymer solution into the cell at constant flow rate. The syringe had a capacity of 250 ml. A photograph of the syringe pump is shown in **Fig. 6.3**.



Fig. 6.3 – Chemyx Nexus Syringe Pump

6.4 Experimental Procedure

Visual cell was tightly packed with dry spherical glass beads followed by saturation with mineral oil. Pore volume (PV) of the porous medium was measured by direct method. Volume of glass beads in the visual cell was subtracted from the bulk volume of the cell. A specific gravity of 2.5 was used for calculating the volume of glass beads.

After the visual cell was packed with glass beads and saturated with mineral oil, the flooding experiments were started. Mineral oil was colored using an inert organic dye to distinguish it from colorless polymer. HPAM samples prepared according to the procedure explained earlier were injected at a constant flow rate

of 0.96 ml/min using a syringe pump. Volumes of effluent collected at regular intervals were recorded. As polymer pushes oil, it creates clearly distinguishable displacement patterns. These images were captured at different time steps using a high resolution digital camera mounted on a tripod. After the breakthrough had occurred, volume of oil and polymer produced were recorded separately. Flooding was continued until either the oil produced was too low or the water cut has risen to 90% or above. Typically flooding was continued until 1.2 to 1.5 PV of polymer was injected.

6.5 Rheological Characterization of HPAM Solutions

Please refer to section 5.1 of the previous chapter for rheological measurements and plots for HPAM-1 to HPAM-4.

6.6 Results and Discussion of Visualization Experiments

Four HPAM solutions with same average molecular weight (same viscosity) but different MWD (different elasticity) were flooded through visual cell to investigate the individual effect of elasticity on oil recovery and to conduct visual analysis on frontal displacement of oil by elastic polymers.

6.6.1 Oil Recovery Performance

Fig. 6.4 shows the cumulative oil produced by four HPAM samples at different pore volumes of polymer injected. From the figure, it is evident that the cumulative oil production at a particular pore volume of polymer injected is

highest in case of HPAM-4 followed by HPAM-3 and HPAM-2, with HPAM-1 yielding the lowest oil recovery. It also shows that, greater volume of polymer was required in case of HPAM-1 and yet the recovery was lowest compared to other solutions. This means that, oil was recovered much earlier at lower water cuts with HPAM-4 than other samples.

Table 6.1 summarizes the breakthrough and total recoveries after polymer flooding.

Table 6.1 - Overall and Breakthrough recoveries after HPAM flooding		
HPAM Samples	% Breakthrough Recovery	% Total Recovery
HPAM 1	48.70	80.52
HPAM 2	64.94	81.17
HPAM 3	66.45	84.87
HPAM 4	73.68	90.13

Table 6.1 shows percentage oil recovery at breakthrough time and at the end of the flooding experiment. As seen in **Table 6.1** as well as in **Fig. 6.4** and **Fig 6.5**, there is a large difference in recovery values among different HPAM samples. HPAM-1 in particular had a very early breakthrough with oil recovery being less than 50% of OOIP. Breakthrough occurred at much later stages for HPAM 2, 3 and 4. HPAM-4, being the most elastic among all samples, had the longest breakthrough time and highest recovery at breakthrough time and at the end of flooding.

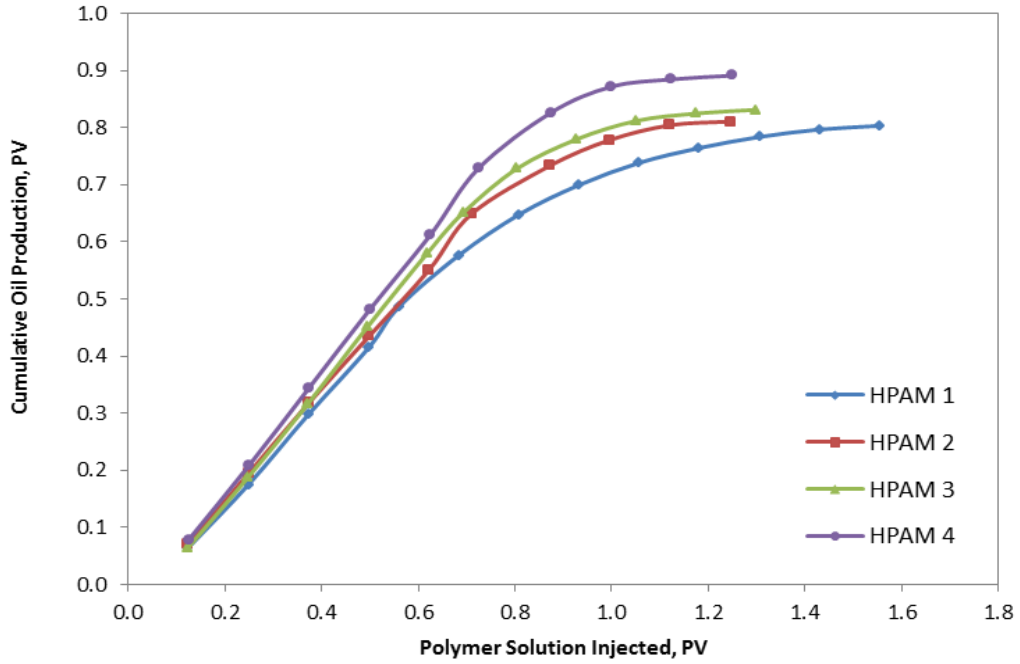


Fig. 6.4 - Cumulative oil produced vs. pore volume of polymer injected

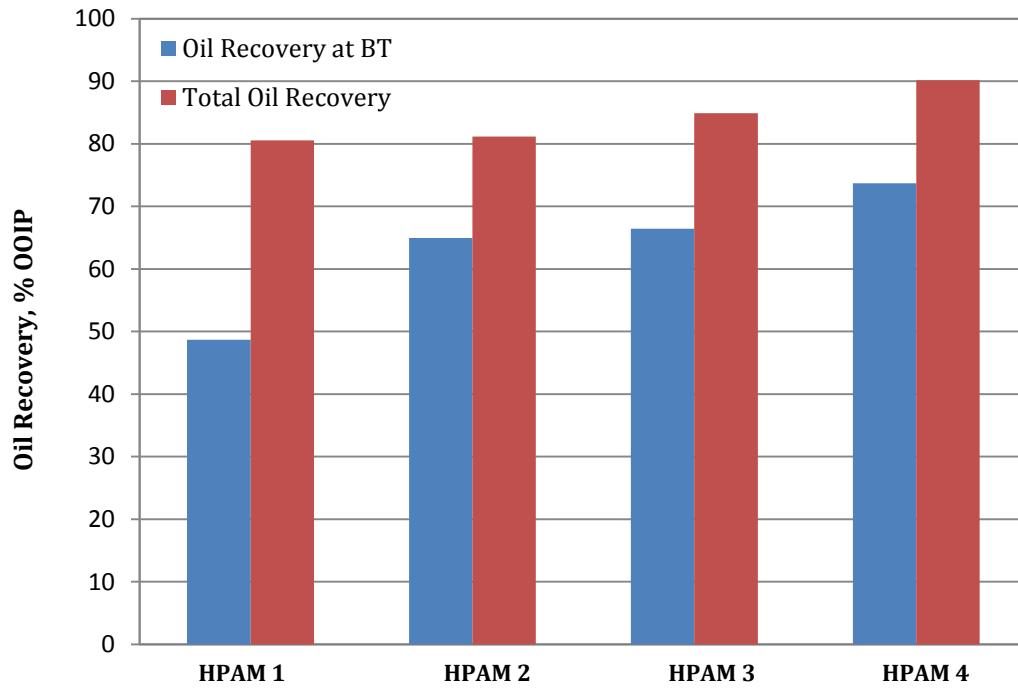


Fig. 6.5 - Breakthrough recovery and overall oil recovery after polymer flooding

In all four cases, it was observed that the rate of oil production dropped after breakthrough has occurred. Since all four HPAM samples had the same average molecular weight (or shear viscosity), HPAM-4 polymer yielding ~10% higher recovery after 1.2 PV of polymer injection than HPAM-1 can be attributed to their difference in elasticity. As indicated in chapter 5, the elastic modulus of HPAM-4 is 16 times greater than that of HPAM-1 at an angular frequency of 0.1 rad/s and 3 times greater at an angular frequency of 1 rad/s.

6.6.2 Visual Analysis

Displacement patterns shown in **Fig. 6.6** explain the mechanism during propagation of polymer as it displaces the oil phase at different stages during the course of flooding. These photographs compare the displacement fronts created by four HPAM solutions at eight different pore volumes of polymer injected. Different flow patterns were observed depending upon the elasticity of the polymer solution injected.

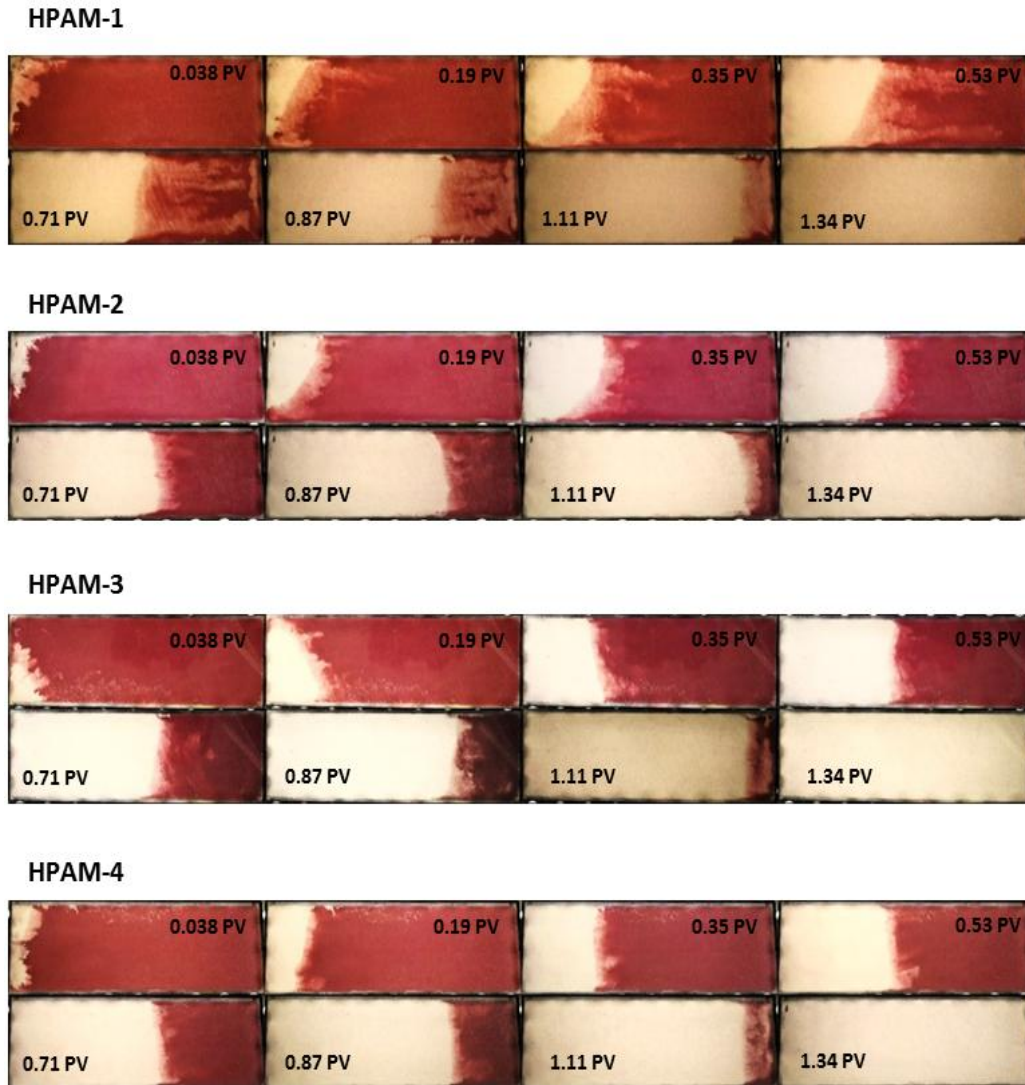


Fig. 6.6 - Displacement fronts for polymer flooding at different pore volumes of polymer injected

Magnified images of displacement fronts showed in **Fig. 6.7(a)** and **Fig. 6.7(b)** give a good account on how the fronts are propagating. The dark red color zone shows completely oil saturated region. The light red regions are partially unswept oil zone while the white color region is almost completely swept by polymer.

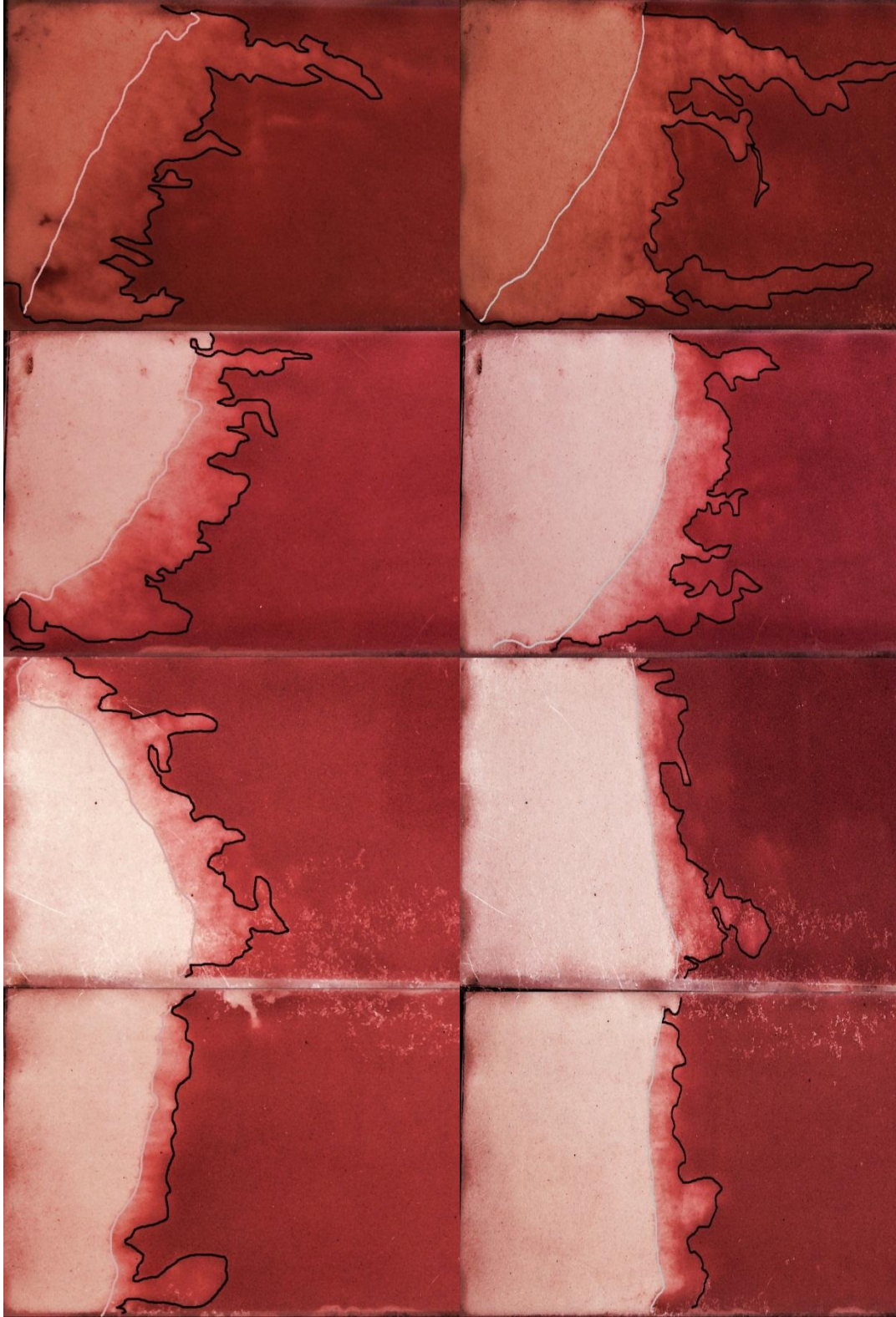


Fig. 6.7(a) - Magnified portion of displacement fronts after injecting 0.19 PV (Left) and 0.35 PV (Right) of polymer solution

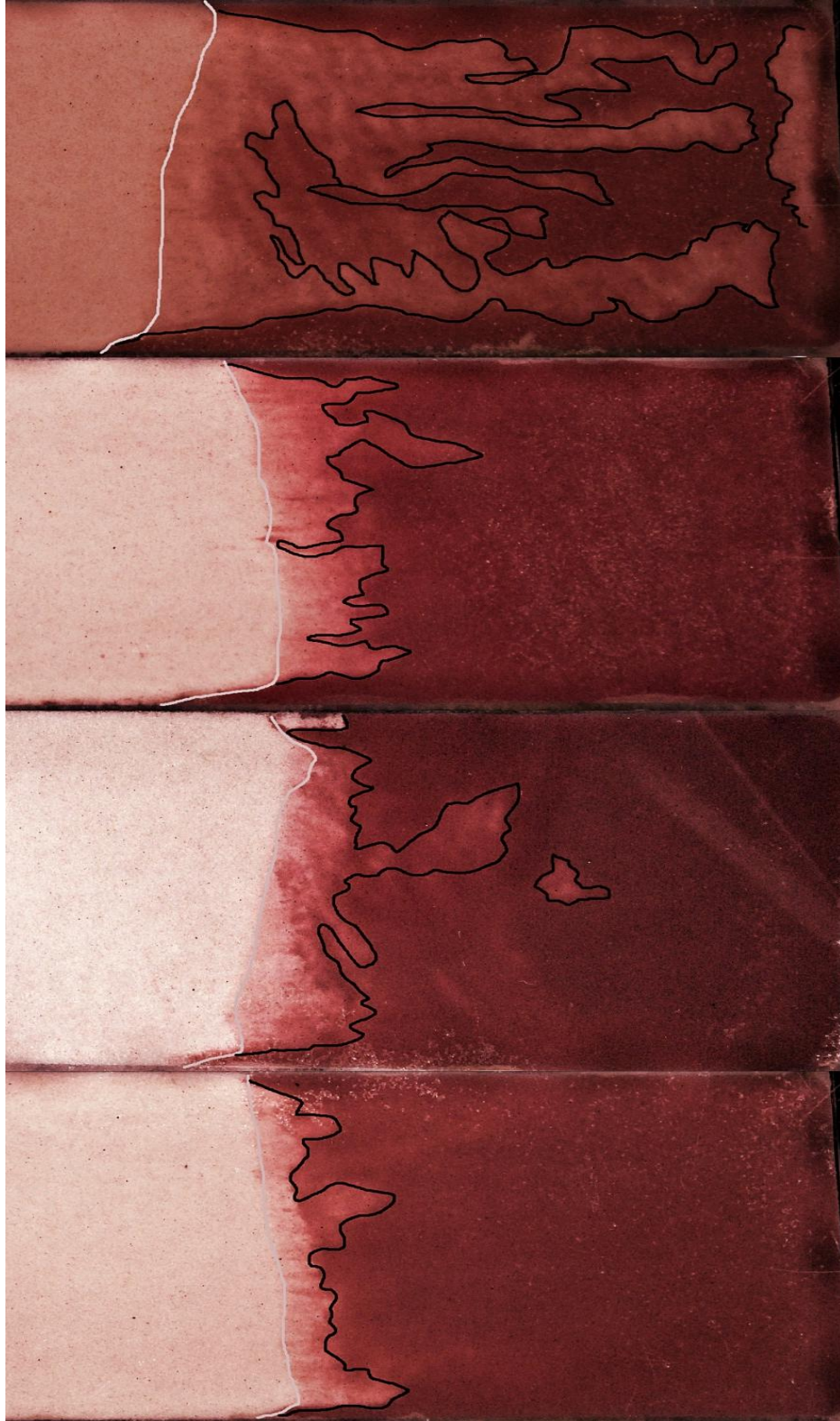


Fig. 6.7(b) - Magnified portion of displacement fronts after injecting 0.71

PV of polymer solution

As flooding continued, two distinct zones were observed for all four polymers (HPAM-1 to HPAM-4) as marked in **Fig. 6.7**. The first one is a partially swept zone with variable degree of fingering depending on the polymer type and characterized by the front propagating forward, shown by black lines while other one is a more stable zone characterized by the stable front left behind, shown by white lines. Behind the fingering zone (propagating front) is the water, which flows without any instabilities. Similar observations were made by Riaz and Tchelepi (2008) during their numerical simulations.

As the polymer flood moves through the oil saturated region of the visual cell towards the producer, the propagating front shows development of fingers. The degree of development of these fingers at any time during the flooding process (or at any pore volume of polymer injected) varies for each polymer samples studied. **Fig. 6.7(a)** and **Fig. 6.7(b)** show the comparative development of propagating and stable front phenomena after 0.2 PV, 0.35 PV and 0.7 PV of polymer injection, respectively. Less finger initialization was observed in the case of HPAM-3 and HPAM-4 compared to that seen for HPAM-1 and HPAM-2. As flooding continued, the number of fingers and the length of each finger increased in the propagating front for HPAM-1 and HPAM-2, whereas the finger initiation was dampened ahead of propagating front for HPAM-3 and HPAM-4.

The area between the forward moving propagating front and the stable front leaving behind is a good measure of overall stability and the performance. More

closely and parallel these two fronts move in the reservoir, higher the swept area by polymer (stable zone area) and higher the performance in terms of breakthrough recovery. This area was larger for HPAM-1 than that for HPAM-2 due to large fingers. Therefore, the polymer propagating front breaks through just around 0.56 PV during HPAM-1 polymer flooding and resulted in less than 50% of recovery, whereas the breakthrough for HPAM-2 polymer occurred after 0.71 PV injection and the recovery at breakthrough was almost ~15% higher at 64.94%. The difference in these two polymers was only in their elastic properties (**Fig. 5.4**). This resulted in different propagating front and stable front profile between HPAM-1 and HPAM-2.

In case of HPAM-3 and HPAM-4, polymer elasticity has further enhanced the performance by minimizing the fingers in the propagating front. The breakthrough for HPAM-3 and HPAM-4 was observed at 0.71 PV and 0.75 PV respectively. As seen in **Fig. 6.7**, the forward moving propagating front and stable front moves almost parallel and close to each other for HPAM-4, having the highest elasticity. This can be considered as the most stable form of displacement among all four HPAM samples. Also, it can be noted that the area swept by polymer (area of the stable zone) at a given point of time is greater in case of HPAM-4 followed by HPAM-3, HPAM-2 and HPAM-1, in the order of decreasing elastic nature.

The overall recovery depends on the oil swept in the stable zone left behind. The lighter red color in the swept areas (stable zone) for HPAM-1 and HPAM-2 indicate that the residual oil saturation is higher than other HPAM samples at any given time during the flood. This resulted in lower overall recovery of 80.52% and 81.17% for lower elastic polymers HPAM-1 and HPAM-2 respectively compared to 90.13% for highest elastic polymer HPAM-4.

CHAPTER 7

CONCLUSIONS AND RECOMMENDATIONS

7.1 Conclusions

Three main objectives were set at the beginning of this research study:

1. To devise a screening criteria for selecting polymers for EOR
2. To study the individual effect of elasticity of polymers on improved oil displacement efficiency
3. To establish visual conformance of the role of elasticity of viscoelastic polymers on enhanced oil recovery

These objectives were successfully achieved through experimental study conducted. Results from these experiments were summarized and following conclusions were drawn:

- A rheological characterization study of polymer solutions in association with polymer flooding experiments was conducted as part of the efforts to develop a systematic approach for selecting best polymer for polymer flooding operations.
- Radial core experiments were conducted with HPAM samples having same average molecular weight (same viscosity) but different elastic modulus. Polydispersity index – a measure of elasticity – can be used to screen a polymer among available same average molecular weight polymers for better EOR performance.

- The cumulative and breakthrough oil recovery analysis provided a good measure of polymer screening based on MWD and average molecular weights of polymers. Results from the radial core flooding experiments show that higher recovery can be achieved with polymers having higher elasticity.
- The amount of polymer required to produce a fixed pore volume of oil is also correlated well with the elasticity of polymer solution. The higher the elasticity of HPAM sample, the lower the volume of HPAM solution needed to be injected to produce a fixed volume of oil.
- Rheological characteristics of polymer solutions before and after flooding experiments were found to be significantly different. As a result of progressive change in polymer rheology, effective oil recovery goes down with PV of polymer injected. The degree of viscosity and elasticity reduction during the course of flooding depends on both average molecular weight and molecular weight distribution and influences the oil recovery efficiency.
- Results have shown that average molecular weight by itself might not be the best criteria to select optimum polymer fluid composition for water flooding operations. Considering the molecular weight distribution (polydispersity index) together with average molecular weight seems to

be the better approach for formulating optimum polymer solutions with higher oil recovery performance at lower polymer concentrations (i.e., lower cost).

- Visual study of polymer flooding experiments provided an insight into the frontal displacement patterns of polymer solutions with different elasticity. The visualization results confirmed that higher elastic polymers are better suited for achieving higher sweep efficiency with stable displacement fronts.
- Different viscous fingering patterns were obtained depending on the elasticity of polymer injected.
- As polymer pushed ahead through the porous media, two distinct zones were observed: the first one was a partially swept zone with variable degree of fingering depending on the polymer type, characterized by the front propagating forward, while other one was a more stable zone characterized by more stable fronts.
- The degree of development of fingers at any time during the flooding process varies for each polymer sample depending on their elasticity values. Less finger initialization was observed in the case of polymers with higher elasticity compared to that seen for lower elastic polymers.
- As flooding continued, the number of fingers and the length of each finger increased in the propagating front for polymers with low elasticity,

whereas the finger initiation was dampened ahead of propagating front for higher elasticity polymers.

- The area between the forward moving propagating front and the stable front leaving behind is a good measure of overall stability and performance. If these two fronts propagate closely and parallel to each other, higher breakthrough recovery performance can be achieved.
- Higher elastic polymers help achieve better volumetric sweep efficiency and displacement efficiency by reducing the residual oil saturation in the swept zones.
- Mechanism of viscous fingering in two-phase horizontal immiscible flow system has been visually explained in terms of elasticity of polymers.

7.2 Recommendations

Although most of the objectives set were achieved, there is still scope for further research and are recommended here:

- Number average molecular weight (M_n) of polymer grades needs to be found out (by using GPC/SEC and other techniques) in order to calculate polydispersity index of polymer solutions. This will enable polymer solutions to be compared in a better way.
- Rheological measurements of polymer effluent samples after the flooding experiments alone may not be sufficient enough to draw conclusions regarding polymer degradation, adsorption on rock surfaces. Polymer concentration must be measured before and after the flooding experiments and compared for a better understanding of the mechanism of degradation/adsorption of polymers.
- The conclusions drawn from the flooding experiments are based on polymer injection as a secondary recovery method. Few experiments can be performed with waterflooding followed by polymer flooding to quantify secondary and tertiary recovery performance and analyze the effect of elasticity on tertiary recovery.
- All the experiments were carried out at room temperature and deionized water was used for polymer solution preparation. Effect of salt, alkali and

other parameters on solution properties of polymers must be studied and how these factors affect the oil recovery performance together with elasticity must be determined experimentally.

- Experiments needs be conducted with heavy oil samples from field using high concentration polymer solutions. AP flood, ASP floods can be tried on heavy oil displacement experiments to understand the effect of elasticity under those conditions.

REFERENCES

- Abdel-Khalik, S. I., Hassager, O., and Bird, R. B. 1974. "Prediction of Melt Elasticity from Viscosity Data". *Polym. Eng. Sci.*, **14(12)**: 859-867
- Abou-Kassem, J. H., and Farouq Ali, S. M. 1986. "Flow of Non-Newtonian Fluid in Porous Media". SPE 15954, Eastern Regional Meeting, Columbus, Ohio, USA, 12-14 November
- Ait-Kadi, A., Carreau, P. J., and Chauveteau, G. 1987. "Rheological Properties of Partially Hydrolyzed Polyacrylamide Solutions". *J. of Rheology*. **31(7)**: 537-561
- Akstinat, M. H. 1980. "Polymers for Enhanced Oil Recovery in Reservoirs of Extremely High Salinities and High Temperatures". SPE 8979, Fifth International Symposium on Oilfield and Geothermal Chemistry, Stanford, CA, 28-30 May
- Aktas, F., Clemens, T., Castanier, L. M., and Kovscek, A. R. "Viscous Oil Displacement with Aqueous Associative Polymers". SPE 113264, SPE/DOE Symposium on Improved Oil Recovery, Tulsa, OK, USA, 20-23 April
- Aldasani, A., and Bai, B. 2010. "Recent Developments and Updated Screening Criteria for Enhanced Oil Recovery Techniques". SPE 130726, CPS/SPE International Oil and Gas Conference and Exhibition, Beijing, China, 8-10 June
- Anonymous, "Husky Energy Implements Alkaline-Surfactant-Polymer Flood Technology". *New Technology Magazine*, Daily News, October 16, 2006
- Armstrong, T. A., 1967. "Polymer Floods Attacking Recovery Gap", *Oil and Gas Journal*, **65(1)**: 46-48

Bai, Y., Zhang, X., and Zhao, G. 2011. "Theoretical Analysis of Microscopic Oil Displacement Mechanism by Viscoelastic Polymer Solution". *Theoretical & Applied Mechanics Letters*, **1(2)**: 1-4

Bird, R. B., Stewart, W. E. and Lightfoot, E. N. 1960. "*Transport Phenomena*". Wiley, New York

Bird, R. B., Hassager, O., and Abdel-Khalik, S. I. 1974. "Co-Rotational Rheological Models and the Goddard Expansion". *AIChE J.*, **20(6)**: 1041-1066

Bird, R. B., Armstrong, R. C. and Hassager, O. 1987. "*Dynamics of Polymeric Liquids*". Vol. 1 *Fluid Mechanics*, 2nd Edition, John Wiley and Sons, Chichester

Buchgraber, M., 2008. "Determination of the Reservoir Behavior of Associative Polymers at Various Polymer Concentrations". MSc Thesis, University of Leoben, Austria

Buckley, S. E., and Leverett, M. C. 1942. "Mechanisms of Fluid Displacement in Sands", *Trans. AIME* **146**: 107-116.

Burick, E. J., 1968. "What, Why and How of Polymers for Waterflooding", *Pet. Eng.*, **40(8)**: 60-64

Cannella, W. J., Huh, C., and Seright, R. S. 1988. "Prediction of xanthan Rheology in Porous Media". SPE 18089, Annual Technical Conference and Exhibition, Houston, Texas, 2-5 October

Caram, Y., Bautista, F., and Puig, J. 2006. "On the Rheological Modeling of Associative Polymers". *Rheologica Acta*, **46**: 45-57

Chang, L., Zhang, Z. Q., Wang, Q. M., Xu, Z. S., Guo, Z. D., Sun, G. Q., Cao, X. L., and Qiao, Q. 2006. "Advances in Polymer Flooding and Alkaline/Surfactant/Polymer Processes as Developed and Applied in the Peoples' Republic of China". *JPT*, **58(2)**: 84-89

Chauveteau, G. 1981. "Molecular Interpretation of Several Different Properties of Flow of Coiled Polymer Solutions through Porous Media in Oil Recovery Conditions". SPE 10060, 56th Annual Fall Conference, San Antonio, TX, 5-7 October

Chauveteau, G. 1982. "Rod-like Polymer Solution Flow through Fine Pores: Influence of Pore Size on Rheological Behavior". *J. Rheology* **26(2)**: 111-142

Chauveteau, G., and Zaitoun, A. 1981. "Basic Rheological Behavior of Xanthan Polysaccharide Solutions in Porous Media: Effect of Pore Size and Polymer Concentration". Proceedings of the First European Symposium on EOR, Bournemouth, England, September

Chouke, R.L., van Meurs, P., and van der Poel, C. 1959. "The Instability of Slow, Immiscible, Viscous Liquid-Liquid Displacements in Permeable Media". *Trans., AIME* **216**, 188-194

Christopher, R.H., and Middleman, S. 1965. "Power-Law Flow through a Packed Tube". *Ind. Eng. Chem. Fund.* **4(4)**: 422-426

Clay, T.D., and Menzie, D.E. 1966. "The Effect of Polymer Additives on Oil Recovery in Conventional Waterflooding". SPE 1670, Four Corners Regional Meeting, Farmington, New Mexico, 9-10 September

Clifford, P. J., and Sorbie, K. S. 1985. "The Effects of Chemical Degradation on Polymer Flooding". SPE 13586, International Symposium on Oilfield and Geothermal Chemistry, Phoenix, AZ, 9-11 April

Collison, M. 2007. "Good to the Last Drop". *Oil Week*, June

Cosse, R. 1993. "*Basics of Reservoir Engineering*". Institut Francais Du Petrole, t-Editions Technip, Paris, France

Craft B. C., Hawkins M. F., and Terry R. E. 1991. "*Applied Petroleum Reservoir Engineering*". Second Edition. Englewood Cliffs, N. J: Prentice Hall PTR 4-6. 376-384

Craig, F. F. 1971. "*The Reservoir Engineering Aspects of Waterflooding*". SPE Monograph Series No. 3. Richardson, Texas

Davison, P., and Mentzer, E. 1980. "Polymer Flooding in North Sea Reservoirs". SPE 9300, 55th Annual Fall Conference, Dallas, TX, 21-24 September

De Gennes, P. G. 1974. "Coil-Stretch Transition of Dilute Flexible Polymers Under Ultrahigh Velocity Gradients". *J. Chem. Phys.* **60(12)**: 5030-5042

Dehghanpour, H.A., and Kuru, E. 2009. "A New Look at the Viscoelastic Fluid Flow in Porous Media - A Possible Mechanism of Internal Cake Formation and Formation Damage Control". SPE 121640, International Symposium on Oil Field Chemistry, the Woodlands, TX, USA, 20-22 April

Delshad, M., Kim, D. H., Magbagbeola, O. A., Huh, C., Pope, G. A., and Tarahhom, F. 2008. "Mechanistic Interpretation and Utilization of Viscoelastic Behavior of Polymer Solutions for Improved Polymer-Flood Efficiency". SPE

113620, SPE/DOE Improved Oil Recovery Symposium, Tulsa, OK, USA, 19-23 April

Du, Y., and Guan, L. 2004. "Field-Scale Polymer Flooding: Lessons Learnt and Experiences Gained During Past 40 Years". SPE 91787, International Petroleum Conference, Puebla, Mexico, 8-9 November

Dullien, F. A. L. 1979. "*Porous Media: Fluid Transport and Pore Structure*", Academic Press, Washington, USA

Dupuis, D., Lewandowski, F. Y., Steiert, P., and Wolff, C. 1994. "Shear-Thickening and Time-Dependent Phenomena: The Case of Polyacrylamide Solutions". *J. Non-Newtonian Fluid Mech.* **54(4)**: 11-32

Ferry, J. D. 1980. "*Viscoelastic Properties of Polymers*". New York: John Wiley & Sons, Inc.

Garrouch, A.A. 1999. "A Viscoelastic Model for Polymer Flow in Reservoir Rocks". SPE 54379, Asia Pacific Oil and Gas Conference and Exhibition, Jakarta, Indonesia, 20-22 April

Garrouch, A.A., and Gharbi, R.B. 2006. "A Novel Model for Viscoelastic Fluid Flow in Porous Media". SPE 102015, Annual Technical Conference and Exhibition, San Antonio, Texas, 24-27 September

Gleasure, R. W., and Phillips, C. R. 1990. "An Experimental Study of Non-Newtonian Polymer Rheology Effects on Oil Recovery and Injectivity". *SPE Res. Eng.* **5(4)**: 481-486

Gogarty, W. B., 1967. "Mobility Control with Polymer Solutions", *Soc. Pet. Eng. J.*, **7(6)**: 161-173

- Guo, S. 1990. "Physical Chemistry of Seepage", Science Press, Beijing
- Haas, R., and Durst, F. 1981. "Viscoelastic Flow of Dilute Polymer Solutions in Regularly Packed Beds". *Rheol. Acta.* **21**: 566-571
- Han, X. Q., Wang, W.Y., and Xu, Y. 1995. "The Viscoelastic Behavior of HPAM Solutions in Porous Media and Its Effects on Displacement Efficiency". SPE 30013, International Meeting on Petroleum Engineering, Beijing, PR China, 14-17 November
- Heemskerk, J., Janssen-van Rosmalen, R., Holtslag, R.J., and Teeuw, D. 1984. "Quantification of Viscoelastic Effects of Polyacrylamide Solutions". SPE 12652, SPE/DOE Fourth Symposium on Enhanced Oil Recovery, Tulsa, Oklahoma, 15-18 April
- Hirasaki, G. J., and Pope, G. A. 1974. "Analysis of Factors Influencing Mobility and Adsorption in Flow of Polymer Solution through Porous Media". *SPE Journal*, **14(4)**: 337-346
- Homsy, G. M. 1987. "Viscous Fingering in Porous Media". *Ann. Rev. Fluid Mech.* **19**, 271-311
- Hu, Y., Wang, S. Q., and Jamieson, A. M. 1994. "Rheological and Rheoptical Studies of Shear-Thickening Polyacrylamide Solutions". *Macromolecules.* **28(6)**: 1847-1853
- Jennings, R. R., Rogers, J. H., and West, T. J. 1971. "Factors Influencing Mobility Control by Polymers". *JPT*, **23(3)**: 391-401

Jerauld, G.R., Davis, H.T., and Scriven, L.E. 1984. "Stability Fronts of Permanent Form in Immiscible Displacement". SPE 13164, Annual Technical Conference and Exhibition, Houston, Texas, USA, 16-19 September

Jiang, H., Wu, W., Wang, D., Zeng, Y., Zhao, S., and Nie, J. 2008. "The Effect of Elasticity on Displacement Efficiency in the Lab and Results of High Concentration Polymer Flooding in the Field". SPE 115315, Annual Technical Conference and Exhibition, Denver, Colorado, 21-24 September

Kalifa, O., and Aluhwal, H. 2008. "Simulation Study of Improving Oil Recovery by Polymer Flooding in a Malaysian Reservoir". Master of Engineering Thesis, Universiti Teknologi Malaysia

Kaminsky, R.D., Wattenbarger, R.C., Szafranski, R.C., and Coutee, A.S. 2007. "Guidelines for Polymer Flooding Evaluation and Development". IPTC 11200, International Petroleum Technology Conference, Dubai, U.A.E., 4-6 December

Kumar, M., Hoang, V., Satik, C., and Rojas, D. 2008. "High-Mobility-Ratio-Waterflood Performance Prediction: Challenges and New Insights", *SPE* **11(1)**: 186-196

Lake, L. W. 1989. "*Enhanced Oil Recovery*". Englewood Cliffs, New Jersey: Prentice Hall

Lara-Ceniceros, A., Rivera-Vallejo, C., and Jimenez-Regalado, E. 2007. "Synthesis, Characterization and Rheological Properties of Three Different Associative Polymers Obtained by Micellar Polymerization". *Polymer Bulletin*, **58**: 425-433

Lindley, J. 2001. "Chemical Flooding (Polymer)". <http://www.netl.doe.gov>

Littmann, W. 1988. *“Polymer Flooding”*. Amsterdam: Elsevier Science Publishers B.V.

Lozanski, W. R., and Martin, I. 1970. “Taber South – Canada’s First Polymer Flood”. *JCPT*, **9(2)**: 99-106

Lu, X., Wang, Y., and Zhang, Y. 2006. “Strategies and Techniques for a Giant Sandstone Oilfield Development: A Road Map to Maximize Recovery”. Paper SPE 100942 presented at the SPE Asia Pacific Oil & Gas Conference and Exhibition, Adelaide, Australia, September 11-13

Lyons, W. C. 2009. *“Working Guide to Reservoir Engineering”*. Gulf Publishing Company, Burlington, MA, USA

Magueur, A., and Moan, M. 1985. “Effect of Successive Contractions and Expansions on the Apparent Viscosity of Dilute Polymer Solutions”. *Chem. Eng. Comm.* **36(6)**: 351-356

Masuda, Y., Tang, K., Miyazawa, M., and Tanaka, S. 1989. “1D Simulation of Polymer Flooding Including the Viscoelastic Effect of Polymer Solution”. SPE 19499, Asia-Pacific Conference, Sydney, Australia, 13-15 September

McKinley, R. M., John, H. O., and Harris, W. W. 1966. “Non-Newtonian Flow in Porous Media”. *AIChE Journal*, **12(1)**: 17-20

Menard, H. W. 1981. “Toward a Rational Strategy for Oil Exploration”. *Scientific American*, January, **244(1)**: 47-57

Meng, L. W., Kang, W. L., Zhou, Y., Wang, Z. W., Liu, S. R., and Bai, B. J. 2008. “Viscoelastic Rheological Property of Different Types of Polymer

Solutions for Enhanced Oil Recovery”. *J. Cent. South Univ. Technol.* **15(1)**: 126-129

Needham, R. B., and Doe, P. H. 1987. “Polymer Flooding Review”, *J. Pet. Tech.*, **39(12)**: 1503-1507

Neil, J. D., Chang, H. L., and Geffen T. M. 1983. “Waterflooding and Improved Waterflooding in Improved Oil Recovery”. Oklahoma City. Interstate Oil Compact Commission. 1-52

Odell, J. A., and Keller, A. 1986. “Flow-Induced Chain Fracture of Isolated Linear Macromolecules in Solution”. *J. Polym. Sci.* **24(9)**: 1889-1916

Pancharoen, M. 2009. “Physical Properties of Associative Polymer Solutions”. MSc Thesis, Stanford University, Stanford, CA, USA

Pavone, D. “Observations and Correlations for Immiscible Viscous-Fingering Experiments”. *SPEERE*, **7(2)**: 187-194

Pitts, M. J., Campbell, T. A., and Surkalo, H. 1995. “Polymer Flood at the Rapdan Pool”. *SPEERE*, **10(3)**: 183-186

Pope, G. A. 2011. “Recent Developments and Remaining Challenges of Enhanced Oil Recovery”. R&D Grand Challenges. *Journal of Petroleum Technology*, **63 (7)**: 65-68

Pruess, W. K., and Witherspoon, P. A. 1991. “Displacement of a Newtonian Fluid by a Non-Newtonian Fluid in a Porous Medium”. *Transport in Porous Medium*, **6(2)**: 115-142

Pye, D. J., 1964. "Improved Secondary Recovery by Control of Water Mobility", *J. Pet. Tech.*, **16(8)**: 911-916

Ranjbar, M., Rupp, J., Pusch, G., and Meyn, R. 1992. "Quantification and Optimization of Viscoelastic Effects of Polymer Solutions for Enhanced Oil Recovery". SPE 24154, SPE/DOE Eighth Symposium on Enhanced Oil Recovery, Tulsa, Oklahoma, 22-24 April

Riaz, A., and Tchelepi, H. A. 2008. "Dynamics of Vertical Displacement in Porous Media Associated with CO₂ Sequestration". *SPE Journal*, **13(3)**: 305-313

Roche, P. 2010. "As CO₂ EOR Stalls, Polymer Floods Ramp Up". *New Technology Magazine*, December

RP 63, "Recommended Practices for Evaluation of Polymers used in Enhanced Oil Recovery Operations". First Edition. 1990. Washington DC: API

Sandiford, B. B., 1969. "Laboratory and Field Studies of Waterfloods Using Polymer Solutions to Increase Oil Recovery", *J. Pet. Tech.*, **16(8)**: 917-922

Savins, J. G. 1969. "Non-Newtonian Flow through Porous Media". *Industrial and Engineering Chemistry*, **61(10)**: 18-47

Seright, R. S. 1991. "Effect of Rheology on Gel Placement". *SPE* **6(2)**: 212-218; *Trans.*, AIME, **291**

Seright, R. S. 2010. "Potential for Polymer Flooding Reservoirs with Viscous Oils". SPE 129899, Improved Oil Recovery Symposium, Tulsa, OK, USA, 24-28 April

Shaw, M. T., and McKnight, W. J. 2005. “*Introduction to Polymer Viscoelasticity*”. Third Edition, New York: John Wiley & Sons

Shaw, R. A., and Stright, D. H. 1977. “Performance of Taber South Polymer Flood”. *JCPT*, **16(1)**: 35-40

Shehata, A. M., Ghatas, A., Kamel, M., Aly, A., and Hassan, A. 2012. “Overview of Polymer Flooding (EOR) in North Africa Fields – Elements of Designing a New Polymer/Surfactant Flood Offshore (Case Study)”. SPE 151952, North Africa Technical Conference and Exhibition, Cairo, Egypt, 20-22 February

Sheu, W. S. 2001. “Molecular Weight Averages and Polydispersity of Polymers”. *Journal of Chemical Education*, **78(4)**: 554-555

Shupe, R. D. 1981. “Chemical Stability of Polyacrylamide Polymers”, *J. Pet. Tech.*, **33(8)**: 1513-1529

Singhal, A. “Preliminary Review of IETP Projects Using Polymers”. Prepared for Alberta Energy and Alberta Innovates-Energy and Environment Solutions, Public Release July 1, 2011

Sorbie, K.S. 1991. “*Polymer-Improved Oil Recovery*”. London: Blackie and son limited

Stahl, G. A., and Schulz, D. N. 1988. “*Water Soluble Polymers for Petroleum Recovery*”. Plenum Publishing Corp., New York

Taber, J.J., Martin, F. D., and Seright, R. S. 1997. “EOR Screening Criteria Revisited – Part 1: Introduction to Screening Criteria and Enhanced Recovery Field Projects”. *SPE*, **12(3)**: 189-198

Taber, J.J., Martin, F. D., and Seright, R. S. 1997. “EOR Screening Criteria Revisited – Part 2: Applications and Impact of Oil Prices”. *SPE*, **12(3)**: 199-206

Thurston, G. B., and Pope, G. 1981. “Shear Rate Dependence of the Viscoelasticity of Polymer Solutions”. *Journal of Non-Newtonian Fluid Mechanics*, **9(1)**: 69-78

Urbissinova, T.S., 2010. “Experimental Investigation of the Effect of Elasticity on the Sweep Efficiency in Viscoelastic Polymer Flooding Operations”. MSc Thesis, University of Alberta, Edmonton, AB, Canada

Urbissinova, T.S., Trivedi, J.J., and Kuru, E. 2010. “Effect of elasticity during viscoelastic polymer flooding: A possible mechanism of increasing the sweep efficiency”. SPE 133471, Western North American Regional Meeting, Anaheim, California, USA, 26–30 May

van Poolen, H. K., and Jargon, J. R. 1969. “Steady State and Unsteady State Flow of non-Newtonian Fluids through Porous Media”. *SPE Journal*, **9(1)**: 80-88

Veerabhadrapa, S.K., Urbissinova, T.S., Trivedi, J.J., and Kuru, E. 2011. “Polymer Screening Criteria for EOR Application – A Rheological Characterization Approach”. SPE 144570, Western North American Regional Meeting, Anchorage, Alaska, USA, 7-11 May

Wang, D., Cheng, J., Yang, Q., Gong, W., Li, Q., and Chen, F. 2000. “Viscoelastic polymer can increase micro-scale displacement efficiency in cores”. SPE 63227, Annual Technical Conference and Exhibition, Dallas, Texas, USA, 1-4 October

Wang, D., Cheng, J., Xia., H., Li,Q., and Shi, J. 2001. “Viscous-elastic fluids Can Mobilize Oil Remaining after Water-Flood by Force Parallel to the Oil-Water Interface”. SPE 72123, Asia Pacific Improved Oil Recovery Conference, Kuala Lumpur, Malaysia, 8-9 October

Wang, D., Cheng, J., Junzheng, W., and Gang, W. 2002. “Experiences Learned after Production more than 300 million Barrels of Oil by Polymer Flooding in Daqing Oil Field”. SPE 77693, Annual Technical Conference and Exhibition, San Antonio, Texas, September 29- October 2

Wang, D., Dong, H., Lv, C., Fu, X., and Nie, J. 2008. “Review of Practical Experience of Polymer Flooding at Daqing”. SPE 114342, SPE/DOE Symposium on Improved Oil Recovery, Tulsa, OK, USA, 20-23 April

Wassmuth, R., Arnold, W., Green, K. and Cameron, N. 2009. “Polymer Flood Application to Improve Heavy-Oil Recovery at East Bodo”. *JCPT*, **48(2)**: 55-61

Willhite, G. P. 1986. “*Waterflooding*”. SPE Textbook Series No. 3. Richardson, Texas

Willhite, G. P., and Uhl, J. T. 1986. “Correlation of the Mobility of Biopolymer with Polymer Concentration and Rock Properties in Sandstone”. *Polymeric Science and Engineering*. **55**: 577-581

Wreath, D., Pope, G., and Sepehrnoori, K. 1990. “Dependence of Polymer Apparent Viscosity on the Permeable Media and Flow Conditions”. *In Situ (USA)*, **14 (3)**: 263-284

Xia, H., Ju, Y., Kong, F., and Wu, J. 2004. “Effect of Elastic Behaviour of HPAM Solutions on Displacement Efficiency under Mixed Wettability

Conditions”. SPE 90234, International Petroleum Conference in Mexico, Puebla, Mexico, 8-9 November

Yang, F., Wang, D., Yang, X., Sui, X., Chen, Q., and Zhang, I. 2004. “High Concentration Polymer Flooding is Successful”. SPE 88454, Asia Pacific Oil and Gas Conference and Exhibition, Perth, Australia, 18-20 October

Yang, F., Wang, D., Wang, G., Sui, X., Liu, W., and Kan, C. 2006. “Study on High-Concentration Polymer Flooding to Further Enhance Oil Recovery”, SPE 101202, Annual Technical Conference and Exhibition, San Antonio, Texas, USA, 24-27 September

Yortsos, Y.C., and Huang, A.B. “Linear Stability Analysis of Immiscible Displacement Including Continuous Changing Mobility and Capillary Effect: Part I – Simple Basic Flow Profiles”. *SPE*, **1(4)**: 378-390; *Trans.*, AIME **282**

Zang, Y. H., Muller, R., and Froelich, D. 1987. “Influence of Molecular Weight Distribution of Viscoelastic Constants of Polymer Melts in the Terminal Zone. New Blending Law and Comparison with Experimental Data”. *Polymer*, **28(9)**: 1577-1582

Zhang, Y., Li, C., and Wang, X. 2004. “Discussions on the Technical of String with Back flush for Separate Layers during the Period of Polymer Flooding”. *Oil & Gas Ground Engineering*. **23(9)**: 26-27

Zhang, L. 2007. “Mechanism for Viscoelastic Polymer Solution Percolating through Porous Media”. *J. Hydrodyn. Ser.* **19(2)**: 241–248

Zhang, L., and Yue, X. 2008. “Displacement of Polymer Solution on Residual Oil Trapped in Dead Ends”. *J. Cent. South. Technol.* **15(1)**: 84–87

Zhang, Z., Li, Jiachun., and Zhou, J. 2010. “Microscopic Roles of Viscoelasticity in HPMA Polymer Flooding for EOR”. *Transport in Porous Media*, **86(1)**: 199-214